Hydrogen isotope fractionation of leaf wax *n*-alkanes in southern African soils

Nicole Herrmann [a*1], Arnoud Boom [b], Andrew S. Carr [b], Brian M. Chase [c], Adam G. West [d], Matthias Zabel [a], Enno Schefuß [a]

[a] *MARUM – Center for Marine Environmental Sciences, University of Bremen, Leobener Straße, Bremen, Germany*

[b] *Department of Geography, University of Leicester, University Road, Leicester LE1 7RH, United Kingdom*

[c] *Centre National de Recherche Scientifique, UMR 5554, Institute des Sciences de l'Evolution de Montpellier, Département Paléoenvironnements, Université Montpellier, Bat.22, CC061, Place Eugène Bataillon, 34095, Montpellier, Cedex 5, France*

[d] *Department of Biological Sciences, University of Cape Town, Rondebosch 7701, Western Cape, South Africa*

* Corresponding author.

E mail: nicole.herrmann@uni-hamburg.de (Nicole Herrmann).

ABSTRACT

The hydrogen isotope composition of plant leaf wax (δD_{wax}) has been found to record the isotope composition of precipitation (δD_p). Hence, δD_{wax} is increasingly used for palaeohydrological reconstruction. δD_{wax} is, however, also affected by secondary factors, such as vegetation type, evapotranspiration and environmental conditions, complicating its direct application as a quantitative palaeohydrological proxy. Here, we present δD_{wax} data from soils along vegetation gradients and climatic transects in southern Africa to

[1] present address: Institute for Geology, University of Hamburg, Bundesstraße 55, Hamburg, Germany

investigate the impact of different environmental factors on δD_{wax}. We found that δD_{wax} correlated significantly with annual δD_p (obtained from the interpolated Online Isotopes in Precipitation Calculator data set) throughout the eastern and central South Africa, where the majority of the mean annual precipitation falls during the summer. We found evidence for the effect of evapotranspiration on δD_{wax}, while vegetation change was of minor importance. In contrast, we found that δD_{wax} did not correlate with annual δD_p in western and southwestern South Africa, where most of the annual precipitation falls during winter. Wide microclimatic variability in this topographical variable region, including distinct vegetation communities and high vegetation diversity between biomes as well as a potential influence of summer rain in some locals, likely compromised identification of a clear relationship between δD_{wax} and δD_p in this region. Our findings have implications for palaeoenvironmental investigations using δD_{wax} in southern Africa. In the summer rain dominated eastern and central region, δD_{wax} should serve well as a qualitative palaeohydrological recorder. In contrast, the processes influencing δD_{wax} in the winter rain dominated western and southwestern South Africa remain unclear and pending further analyses potentially constrain its use as palaeohydrological proxy in this region.

Keywords: Compound-specific hydrogen isotopes; Southern Africa; Soils; Plant wax; *n*-Alkanes

1. Introduction

Long chain *n*-alkanes of plant leaf wax, and their compound-specific stable hydrogen isotope composition (δD_{wax}) are widely used as a palaeoenvironmental proxy, providing

insights into past hydrological conditions (e.g. Schefuß et al., 2005; Seki et al., 2009; Niedermeyer et al., 2010; Collins et al., 2013; Kuechler et al., 2013). They are stable over geological time scales (Schimmelmann et al., 2006; Eglinton and Eglinton, 2008) and δD_{wax} in lake surface sediments and soils has been shown to correlate with δD of local precipitation (δD_p; Sachse et al., 2004; Rao et al., 2009; Polissar and Freeman, 2010; Luo et al., 2011; Garcin et al., 2012; Schwab et al., 2015; Tuthorn et al., 2015). However, δD_{wax} has also been shown to be influenced by other factors, such as evapotranspiration or plant growth form, which may bias its signal (e.g. Hou et al., 2008; Feakins and Sessions, 2010a; Seki et al., 2010; Douglas et al., 2012; Kahmen et al., 2013b; Berke et al., 2015). To reliably reconstruct hydrological changes in specific settings it is thus essential to understand the factors affecting δD_{wax} in specific environments.

The primary factor controlling δD_{wax} is the hydrogen isotope composition of precipitation which depends on various environmental processes. These include the intensity of precipitation (amount effect), the distance that moisture has travelled over a continental landmass (continental effect), the altitude effect, condensation temperature (temperature effect) and the global ice volume (ice effect) (Dansgaard, 1964; Gat, 1996; Araguás-Araguás et al., 2000). In detail, the amount effect describes the decrease in δD_p with increasing rainfall amount/intensity and is most pronounced in the tropics and mid-latitudes during the rainy season(Dansgaard, 1964; Rozanski et al., 1993; Worden et al., 2007; Risi et al., 2008). Decreasing δD_p is also caused by air masses moving over land away from their oceanic source due to preferential removal of isotopically enriched precipitation during rainout and isotopically depleted residual. The same process

decreases δD_p during orographic uplift of atmospheric moisture, known as the altitude effect (Dansgaard, 1964; Rozanski et al., 1993). With decreasing temperature, the atmosphere can store less moisture, resulting in greater effective rainfall and therefore greater depletion of δD_p (temperature effect), which becomes a more important effect at mid-to high latitudes (Dansgaard, 1964; Rozanski et al., 1993). Additionally, over longer time-scales the global ice volume affects the isotope composition of mean ocean surface water (Dansgaard, 1964).

As soil water and precipitation are the main sources of plant water, their isotopic signature is taken up by plants in their stem water (e.g. Flanagan and Ehleringer, 1991; Gat, 1996). An additional factor that may then alter leaf water δD is D enrichment due to evapotranspiration, which is most pronounced in arid regions (e.g. Krull et al., 2006; Liu et al., 2006; Kahmen et al., 2013a). Furthermore, apparent hydrogen isotope fractionation (i.e. the difference between δD_p and δD_{wax}) has been shown to vary with vegetation type (e.g. grasses, shrubs; Kahmen et al., 2013b), photosynthetic pathway (Liu and Yang, 2008; Feakins and Sessions, 2010b; Gamarra et al., 2016), leaf shape (Gao et al., 2015) and water use efficiency (Hou et al., 2007a; Liu and Yang, 2008). Some studies show large differences in hydrogen isotope fractionation between source water and leaf wax, with substantially smaller apparent fractionation reported in arid vs. humid climates (e.g Feakins and Sessions, 2010a; Polissar and Freeman, 2010; Smith and Freeman, 2006). Additionally, CAM plants, common in semi-arid and arid environments (Ting, 1985), have been reported to exhibit smaller apparent fractionation than C_3 and C_4 plants (Feakins and Sessions, 2010b). As apparent fractionation, mostly of C_3 vs. C_4 plants, is often used for palaeohydrological reconstruction, the

environmental controls on apparent fractionation in semi-arid to arid regions is of substantial interest

While many studies of leaf wax focus on plants, either in natural environments or greenhouse experiments (e.g. Bi et al., 2005; Sachse et al., 2006; Smith and Freeman, 2006; Hou et al., 2007a; Liu and Yang, 2008; Feakins and Sessions, 2010b; McInerney et al., 2011; Gao et al., 2014, 2015; Feakins et al., 2016) relatively few have systematically investigated the compound-specific stable isotope composition of leaf wax components in soils (Chikaraishi and Naraoka, 2006; Krull et al., 2006; Jia et al., 2008; Luo et al., 2011; Schwab et al., 2015; Zech et al., 2015). As waxes are initially deposited in soils, soils serve as an intermediate reservoir before ultimate deposition in lacustrine or marine archives. Soils therefore, better reflect the integrated source of plant wax for such archives. It is known that certain plant functional types produce a higher amount of leaf wax than others (Diefendorf et al., 2011; Bush and McInerney, 2013; Carr et al., 2014), so the relative contributions of leaf waxes from different plant types may differ significantly from their relative proportions in terms of vegetation cover. It is shown that site averages of plants mitigate the effects of large interspecies variability in δD_{wax} and therefore better reflect source water δD (Feakins and Sessions, 2010a).

The aim of this work is to evaluate the influence of different environmental factors on the δD_{wax} composition of soils from southern Africa. Here, we consider compound-specific δD_{wax} of *n*-alkanes across soils collected along transects in South Africa. These transects cover a wide range of climatic conditions and vegetation types. We compared our data with predicted hydrogen isotope composition of precipitation, obtained from the Online Isotopes in Precipitation Calculator (OIPC; Bowen and Revenaugh, 2003), and

groundwater (West et al., 2014) as well as compound specific $\delta^{13}C$ composition (Herrmann et al., 2016) to address the following questions:

(i) Does δD_{wax} in southern African soils reflect the stable hydrogen composition of precipitation (δD_p)?

(ii) What additional factors influence δD_{wax}?

(iii) What are the implications for (palaeo-)environmental reconstructions utilising δD_{wax} in southern Africa?

2. Study area

2.1. Climate

Southern Africa experiences pronounced precipitation seasonality, and seasonality variability (**Fig. 1**a, c), driven by seasonal changes in large-scale atmospheric and oceanic circulation systems (Tyson and Preston-Whyte, 2000). The eastern and central parts of South Africa receive most (> 66%) of their mean annual precipitation (MAP) between October and March, sourced from the Indian Ocean and brought by tropical easterlies. This is commonly referred to as the summer rainfall zone (SRZ, *sensu* Chase and Meadows, 2007). In contrast, the southwestern margin of South Africa is influenced by frontal systems associated with the westerly storm tracks (Tyson, 1986) and receives > 66% of its MAP during the austral winter. This region is therefore called the winter rainfall zone (WRZ; Chase and Meadows, 2007). Between the WRZ and SRZ, a dynamic transition zone is affected by both tropical and temperate systems and receives a more equitable distribution of precipitation during the year, but with significant inter-annual variability. This zone is often referred to as the year-round rainfall zone (YRZ). Combined with strong variation in precipitation seasonality, South Africa also shows a

pronounced precipitation gradient (**Fig. 1**a) from the arid western margin with very low MAP (ca. 50 mm/yr) increasing to the Drakensberg mountains (ca. 1200 mm/yr) in the east, and peaking at ca. 1700 mm/yr in the northeast of the country. A weaker gradient of increasing rainfall to the southwestern tip (ca. 1100 mm/yr) is also observed (Hijmans et al., 2005). Apart from the pronounced rainfall gradient, the mean annual temperature (MAT) also varies significantly from 5 to 24 °C. Highest temperatures occur in the northwest and northeast, whereas the coldest temperatures are related to higher elevation (> 3000 m above sea level), most notably in the Drakensberg mountains (Hijmans et al., 2005). This interplay of precipitation and temperature leads to general higher aridity in the north-western and central parts vs. southwestern and eastern South Africa.

2.2. Vegetation

Climatic conditions strongly shape the vegetation distribution in South Africa (**Fig. 1**b). The biomes comprise the Desert and Succulent Karoo Biomes in the west, the Fynbos Biome of the Cape, the Afromontane Forest, Thicket and Coastal Forests of the southern and Indian Ocean margins, and the Nama Karoo, Grassland and Savanna Biomes of the interior (Cowling et al., 1997; Mucina and Rutherford, 2006). These biomes are characterised by a variety of plant functional types (Mucina and Rutherford, 2006). Woody C_3 plants and C_3 grasses dominate the Fynbos Biome and in cool, high-altitude grasslands of the Drakensberg Mountains (**Fig. 1**d). In contrast, C_4 grasses dominate the Grassland and Savanna Biomes of the interior (Werger and Ellis, 1981), reflecting increased aridity and particularly high (summer) growing season temperatures (Vogel, 1978; Scott and Vogel, 2000). Plants using crassulacean acid metabolism (CAM), including many succulents, are dominant in arid regions with high rainfall

seasonality, such as in the Succulent Karoo and western Nama Karoo, but also exist in abundance in other biomes (Mooney et al., 1977; Werger and Ellis, 1981).

3. Material and methods

3.1. Sampling

Soil samples were collected in 2010, 2012 and 2013 (**Fig. 1**). Part of the sampling in the Succulent Karoo and Fynbos biomes in 2010 was carried out via a series of 10 x 10 m vegetation survey plots. For the other sites, three samples from a 10-20 m radius were collected, but were not associated with detailed vegetation surveys. Soils from the survey plots were collected from the upper 10 to 15 cm (A horizon with removed litter layer) at four fixed locations within each plot (see Carr et al., 2013).

3.2. Preparation and lipid extraction

The samples were freeze-dried at the University of Leicester and were ground using an agate mortar and pestle after removal of root and stem pieces. They were extracted 3x with an accelerated solvent extractor (ASE200) using 9:1 dichloromethane (DCM) and MeOH at 100 °C, 1000 psi for 5 min. Squalane was added as internal standard in known amount before extraction. Blank samples (combusted sand) contained only trace amounts of lipids. Each total lipid extract (TLE) was concentrated using rotary evaporation. The TLE was separated into hexane-insoluble and hexane-soluble fractions by pipette column chromatography consisting of 4 cm sodium sulphate (Na_2SO_4). The hexane-soluble fraction was saponified with 0.1M KOH in MeOH at 85 °C for 2 h. Neutral compounds were then extracted with hexane. The hydrocarbons were obtained from the neutral fraction via pipette column chromatography consisting of 4 cm of deactivated silica gel (60 mesh, 1% H_2O) using ca. 4 ml of hexane. The hydrocarbons

were separated into unsaturated and saturated hydrocarbon compounds by pipette column chromatography loaded with $AgNO_3$-Si-coated (4 cm) using ca. 4 ml of hexane as solvent.

Some soil samples had high contents of cyclic and branched hydrocarbons, which complicate the identification and separation of individual *n*-alkanes for compound-specific isotope analysis. In these cases urea adduction was carried out to separate *n*-alkanes from cyclic and branched hydrocarbons. To this end, 4.5 ml hexane/DCM (2:1) and 1.5 ml urea solution (40 mg/ml in MeOH) were added to the hydrocarbon fraction and cooled to 4 °C for 15 min and then dried under N_2. Hexane was then added and removed after vortexing for 30 s with a pipette. The procedure was conducted 3 times. MilliQ water was added to dissolve the urea crystals and *n*-alkanes were extracted using hexane/DCM (4:1).

3.3. Instrumental analysis

Quantification of long chain *n*-alkanes was conducted using a ThermoFischer Scientific Focus gas chromatograph equipped with a Rxi-5 ms 30 column (30m, 0.25 mm, 0.25µm), split/splitless injectior operating at 260°C and a flame ionization detector (GC-FID). Helium was used as carrier gas at 1.9 mL min^{-1}. Samples were injected in hexane and the GC temperature was programmed to increase from 60°C (2 min hold) to 150°C with 20°C/min, and then with 4°C/min to 320°C (held for 11 min). An external standard was used for quantification containing *n*-C_{18} to *n*-C_{34} alkanes in known concentration. Repeated analyses of the external standard resulted in a quantification precision of 5 %.

Compound-specific δD analysis of leaf wax *n*-alkanes were carried out using a ThermoFischer Scientific Trace GC equipped with a HP-5 ms column (30 m, 0.25 mm, 1

μm) coupled via a pyrolysis reactor operated at 1420 °C to a ThermoFischer MAT 253 isotope ratio mass spectrometer. Helium was used as carrier gas at 1.2 mL min^{-1}. The samples were injected into a PTV injector at 45°C and then transferred onto the GC column. The GC temperature was programmed to increase from 120°C (3 min hold) to 200°C with 30 °C/min, and then with 4°C/min to 320°C (held for 24 min). All measurements were calibrated against H_2 reference gas (δD = -337 ± 3‰) which δD value was determined by analyses of four IAEA water standards using a ThermoFisher Scientific thermal conversion/elemental analyser. All δD values are given in permil (‰) relative to Vienna Standard Mean Ocean Water (VSMOW). The daily measured H_3^+ factor varied between 5.2 and 5.4 ppm n/A during the analysis period with maximum variation of 0.1 ppm n/A from day to day. A laboratory standard, containing of 15 *n*-alkanes and squalane with known isotopic composition (ranging from -261 to -33‰), was measured before each sample sequence and after every six sample measurements and yielded a long term accuracy and precision of 0 and 2.3‰ (n > 5000), respectively. The laboratory standard was measured routinely against offline-determined standards (mixtures of *n*-alkanes “Arndt B2” from Arndt Schimmelmann, Department of Geological Sciences, Indiana University) with isotopic offsets within analytical error. Data processing was accomplished using Isodat software 3.0. For each samples at least a duplicate measurement was obtained and the averaged precision was 1‰ for the homologues *n*-C_{29} and *n*-C_{31}. The precision of the internal standard (squalane) was 2‰ (n=50). Compound-specific $\delta^{13}C$ values have been reported before (Herrmann et al., 2016).

3.4. Climate data

Site-specific mean annual precipitation (MAP), mean annual temperature (MAT), the seasonality of precipitation and temperature, as well as the monthly and quarterly precipitation and temperature extremes, were obtained from WorldClim 1.4 (Hijmans et al., 2005). The data are based on interpolation of average monthly climate data from weather stations on a 30 arc-second (ca. 1 km²) resolution grid. The aridity index and potential evapotranspiration (PET) data were obtained from the CGIAR-CSI GeoPortal on a 30 arc-second (ca. 1 km²) resolution grid (Trabucco and Zomer, 2009).

3.5. δD of precipitation and groundwater

Annual average and monthly data for δD of precipitation (δD_p) were obtained from the online isotopes in precipitation calculator (OIPC, www.waterisotopes.org, accessed April 2014) using a 10' resolution grid (Bowen and Revenaugh, 2003; Bowen et al., 2005). The data are based on interpolation of the D isotope composition of precipitation obtained from the Global Network for Isotopes in Precipitation (GNIP) database. The 95% confidence interval of interpolated δD_p ranges between 3 and 6‰ for the study area in South Africa (Bowen and Revenaugh, 2003). Note that the coverage of δD_p monitoring weather stations is poor in southern Africa (two stations, one in Pretoria and one in Cape Town), and therefore the accuracy of the interpolated isotope distribution may be limited. A comparison of annual δD_p and MAP along the soil transects revealed a strong negative correlation, suggesting control via the amount effect in the SRZ (r -0.84, $p < 0.001$), whereas annual δD_p and MAP showed a weak correlation in the YRZ (r -0.67, p 0.143) and no correlation in the WRZ (r -0.33, p 0.130; **Fig. 2**). Consistent with this, a 12-yr record from Cape Town (WRZ) showed a weak amount effect and temperature effect (Harris et al., 2010). In contrast δD_p correlates negatively with altitude

in the SRZ and the WRZ (Supplementary material Fig. 1). For further analysis, additional δD values for groundwater were obtained from West et al. (2014). They are based on spatial analysis of measured δD values of groundwater (δD_g) from 369 monitoring locations across South Africa sampled between April 2006 and September 2007 (West et al., 2014). The standard deviation of δD_g ranges between 6.6 and 7.3‰.

4. Results & Discussion

4.1. Source of soil n-alkanes

In an earlier study of the same soil samples (Herrmann et al., 2016) we found a predominance of long-chain *n*-alkanes and CPI values of higher than 4 in most soil samples indicating a terrestrial higher plants origin and a relatively non-degraded state. We also showed that, on average, *n*-alkane distributions and compound-specific $\delta^{13}C$ compositions differ across the individual biomes reflecting their different vegetation types, despite of a large variability of individual samples (Herrmann et al., 2016). Even though we cannot completely rule out an additional input of wind transported leaf waxes, a strong site-by-site correlation between plant and soil wax distributions has previously been shown for the Succulent Karoo and Fynbos soils (Carr et al., 2013, 2014; Herrmann et al., 2016). Further, studies have been shown, that input of aeolian transported material is negligible south of 25°S (Prospero et al., 2002; Dupont and Wyputta, 2003; Eckardt and Kuring, 2005; Vickery et al., 2013). Therefore, we expect that the bulk of soil *n*-alkanes shows a predominant local signal (Herrmann et al., 2016). An additional unknown factor in our studied soils is the residence time of plant wax biomarkers in the soils, which might be very long, i.e. up to millennia, depending on environmental conditions (Conte and Weber, 2002; Drenzek et al., 2007; Kusch et al.,

2010; Galy et al., 2011). Therefore, δD_{wax} potentially incorporates much older δD_p signals. As we have no compound-specific ^{14}C dating for our samples, we cannot rule out large discrepancies of leaf wax ages in the soils. However, radiocarbon dating on bulk total organic carbon of Grassland (location GTC9) and Savanna (location GTC24) soils results in modern ages (post-1950; Herrmann et al., 2016).

For further discussion we focused on the *n*-C_{29} and *n*-C_{31} alkanes as they are typically used for (palaeo-)climatic studies (e.g. Sachse et al., 2006; Aichner et al., 2010) with the latter being the most abundant homologue in our samples (Herrmann et al., 2016). The concentrations for *n*-C_{29} and *n*-C_{31} in all samples are presented in the Supplementary Table and range between 0.05 and 5.3 µg/g dry weight (dw) and 0.2 to 29 µg/g dw for *n*-C_{29} and *n*-C_{31}, respectively. Intra-site variation is between 4.4 µg/g dw (*n*-C_{29}) and 26 µg/g dw (*n*-C_{31}).

4.2. Relationship between δD_{wax}, δD_p and δD_g

δD_{wax} vary from -75 to -151‰ for *n*-C_{29} and -105 to -161‰ for *n*-C_{31} (Supplementary Table). The intra-site variation spanned a range of 1 to 41‰ for *n*-C_{29} and 0 to 30‰ for *n*-C_{31}. We calculated the amount-weighted mean δD_{wax} of both homologues (*n*-C_{29} and *n*-C_{31}) for each soil sample and then the amount-weighted mean of soils from each plot to obtain a vegetation-integrated δD_{wax} signal for each location. For the SRZ, the most negative δD_{wax} values are found for the grassland biome, with a gradual increase further west in the Nama Karoo biome (**Table 1**).

Several studies show a correlation between δD_{wax} and δD_p for different ecosystems (Sachse et al., 2006; Smith and Freeman, 2006; Polissar and Freeman, 2010; Garcin et al., 2012; Berke et al., 2015; Schwab et al., 2015; Feakins et al., 2016).

However, there is no correlation between δD_{wax} and annual δD_p (r -0.12, *p* 0.41), if all locations across this study area are included (**Table 2**). Considering the distinct rainfall zones separately, however, we observe a different picture. In the SRZ δD_{wax} is correlated significantly with annual δD_p (r 0.65, $p < 0.01$) (, **Table 2**), suggesting that δD_{wax} reflects the δD signal of annual precipitation. However, the range (**Table 1**) of δD_{wax} (49‰) is substantially wider than for δD_p (17‰) in the SRZ. In the drier regions of South Africa soil water is likely to be more affected by evaporation, leading to a D enrichment of soil water and therefore D enriched source water for plants. Additionally, earlier studies found D enriched leaf water due to greater leaf transpiration in drier regions (Smith and Freeman, 2006; Aichner et al., 2010; Sachse et al., 2012; Kahmen et al., 2013a, 2013b). As a consequence this combined evapotranspiration leads to higher δD_{wax} composition in drier areas (Smith and Freeman, 2006; Feakins and Sessions, 2010a; McInerney et al., 2011; Douglas et al., 2012; Kahmen et al., 2013a). Therefore the greater range in δD_{wax} than in δD_p is not unexpected.

δD_{wax} values for the WRZ show a gradual increase from the southern Fynbos to the more northern Succulent Karoo biome and a narrower range (**Table 1**) than for the SRZ. Contrary to the SRZ, the area of the WRZ is much smaller, which leads to reduced distance from the moisture source in the Atlantic Ocean and therefore to a slightly narrower range of δD_p (15‰). The WRZ is, however, affected not only by rain bearing systems from the Atlantic Ocean but also by moisture derived from the southeast (Tyson and Preston-Whyte, 2000), which becomes more important for the south-eastern part. This overlap can complicate the assignment of moisture sources. It has been shown that rain generation in frontal systems is complex, and a clear relationship between isotopic

composition and precipitation amount is lacking (Harris et al., 2010). The topography of the WRZ serves to complicate such relationships further with the Cape Fold Mountains a source of much greater topographic/microclimatic variability than the interior. The resulting orographic effects will lead to specific microclimates in mountainous areas of the WRZ, including higher precipitation rates on the windward sides of slopes and lower rates on the leeward sides (Houze, 2012), as well as small scale differences in δD_p composition due to local convection and rainout (Harris et al., 2010), as described for other mountain areas (Holdsworth et al., 1991; Araguás-Araguás et al., 2000; Bowen and Revenaugh, 2003). Such small-scale variations are likely not reflected in the modelled δD_p. These complex and small-scale processes may explain the weak correlation between δD_{wax} and annual δD_p for the WRZ (r -0.48, *p* 0.02) (, **Table 2**). For the driest season (summer months: DJF) we found a weak correlation between δD_{wax} and δD_p (r -0.48, *p* 0.03), corroborating findings that summer rains might be an important water source, at least for some parts of the WRZ (Chase et al., 2015b). This correlation is stronger for Succulent Karoo soils (r -0.58, *p* 0.03), whereas in the Fynbos biome no correlation (r -0.42, *p* 0.26) is observed (**Table 2**). Plants may use water vapour, cloud moisture and fog as additional moisture sources (e.g. Rundel et al., 1991; Soderberg, 2010; West et al., 2012; Matimati et al., 2013). The moisture uptake from water vapour and fog can be nearly equivalent to the amount of precipitation in the Succulent Karoo (Matimati et al., 2013), while cloud moisture adds to moisture uptake in the Fynbos (West et al., 2012) possibly imprint the δD_{wax} signal.

In addition, differences of plant functional types, species and photosynthetic pathways between the Succulent Karoo and Fynbos (Mucina and Rutherford, 2006)

could have an impact on the δD composition of leaf wax components in WRZ soils as different plant types and photosynthetic pathways show different D enrichment factors (e.g. Smith and Freeman, 2006; Hou et al., 2007b; Liu and Yang, 2008; McInerney et al., 2011; Gao et al., 2014; Gamarra et al., 2016). In the YRZ, we observe a correlation between δD_{wax} and δD_p (r 0.82, *p* 0.04), with higher δD_{wax} in the northern (mean -109 ± 5‰) than in the southern (mean -129 ± 3‰) areas (see Supplementary Table). The higher δD_{wax} in the northern areas appears to be an extension of the westward enrichment trend in the SRZ, affirmed by higher precipitation amounts in the northern YRZ from November to April (Hijmans et al., 2005). In contrast, for the southern locations of the YRZ the period of the highest precipitation lasts from March to June/July (Hijmans et al., 2005). Thus, the southern YRZ locations are more affected by winter precipitation and the northern locations by summer precipitation. For this reason we attribute the northern samples from the YRZ to the SRZ and the southern samples to the WRZ in the discussion below. Including these locations in SRZ and WRZ, respectively, improves the correlations for δD_{wax} and annual δD_p in the SRZ (r 0.66, $p < 0.001$) as well as δD_{wax} and δD_p during the driest quarter in the WRZ (r -0.52, $p < 0.01$; **Fig. 3**).

We also compare our δD_{wax} data with δD_g of groundwater. The latter has been suggested to reflect the δD of precipitation (Rozanski, 1985; Kortelainen and Karhu, 2004; West et al., 2014), at least during the main precipitation season (Wassenaar et al., 2009). For the SRZ the relationship between δD_{wax} and δD_g is slightly stronger (r -0.73, $p < 0.001$) than that for δD_{wax} and δD_p, but surprisingly δD_g is inversely correlated with δD_p (**Fig. 4**). The δD_g values are more depleted in the semi-arid than in the wetter regions, contrary to the trend in the OIPC data. Many studies have shown that shallow

groundwater reflects δD_p (e.g. Kortelainen and Karhu, 2004; Rozanski, 1985; Wassenaar et al., 2009), and here this is apparent for the WRZ (**Fig. 4**; Diamond, 2014). In contrast, in the arid regions of southern Africa, groundwater may be deeper (de Vries et al., 2000; Musekiwa and Majola, 2013), and out of the reach of roots. It may also incorporate older water, that could carries an isotopic signature different from modern precipitation (de Vries et al., 2000). The implication is therefore that plants in arid parts of the SRZ use water immediately from precipitation events and that the OIPC provides the most useful δD data of the plants' water source, in the present absence of other data, for interpretations of δD_{wax}.

4.3. Apparent fractionation factor (ε_{app}) for plant wax derived n-alkanes in soils

To evaluate the influence of vegetation and other environmental factors, e.g. precipitation, aridity and temperature, on the δD_{wax} composition, we calculate the apparent fractionation (ε_{app}) between δD_{wax} and δD of precipitation during the growing season (δD_{pgs}) as:

$$\varepsilon_{app} = \left(\frac{\delta D_{wax} + 1000}{\delta D_{pgs} + 1000} - 1\right) * 1000$$

The δD_{pgs} was calculated as amount-weighted mean of the monthly δD_p values from OIPC. As the seasonality of rainfall is responsible for the water availability and δD_{wax} well reflects δD_p of the growing season in semiarid regions (Niedermeyer et al., 2016), we assume a limited recharge of soil water and plant growth during the non-growing season and, therefore, a limited bias of δD_{wax} towards the non-growing season. To determine the length of growing season for each location we used the definition of the

Food and Agriculture Organization of the United Nations (FAO), defined as the period where the precipitation exceeds half of the potential evapotranspiration:

$$Growing\ season: \frac{precip_x}{PET_x} \geq 0.5$$

where x represents the individual month. For some locations, especially in the Nama Karoo, this definition results in a growing season of zero months. Therefore, we used the month with the highest precipitation/PET ratio as growing season in such cases.

Like δD_{wax}, ε_{app} shows a wide variability, ranging from -83 to -141‰ (**Fig. 5**) with individual uncertainties of 0 to 11‰ (Supplementary Table). The smallest ε_{app} is observed for the Nama Karoo biome and the largest are measured in the Fynbos and Grassland biomes (**Fig. 5**). The ε_{app} becomes smaller with distance from the Atlantic and Indian Ocean moisture sources (**Fig. 5**). In general, there is less apparent fractionation for plants contributing to the soils located in more arid regions of the SRZ compared to more humid parts of the SRZ (**Fig. 6**), The overall SRZ correlation between ε_{app} and MAP is strong (r -0.75, $p < 0.001$; **Fig. 7**) as is the correlation between ε_{app} and precipitation during the growing season (r -0.75, $p < 0.001$;**Table 3**, Supplementary material Fig. 2). On average, less apparent fractionation occurs in the summer rainfall biomes compared with the winter rainfall dominated biomes (two-tailed student's test: $p < 0.001$; **Fig. 6**). Our general observation of lower apparent fractionation for drier environments of the SRZ is similar to other studies in arid regions (Smith and Freeman, 2006; Feakins and Sessions, 2010a; Kahmen et al., 2013a; Berke et al., 2015). By contrast, no correlation is observed between ε_{app} and MAP (**Fig. 7**) or ε_{app} and growing season precipitation for the WRZ (Supplementary material Fig. 2), even if Fynbos and

Succulent Karoo biomes are considered separately (**Table 3**, Supplementary material Fig. 3). This suggests imprints other than solely precipitation amount on ε_{app}.

4.4. Factors influencing deuterium fractionation of leaf wax components in southern Africa

We compare ε_{app} with other environmental data (i.e. aridity, altitude, temperature, PET, $\delta^{13}C_{wax}$) to evaluate their imprints on δD_{wax} composition and apparent fractionation. **Table 3** gives an overview of the relationships between ε_{app} and environmental parameters divided into the different rainfall zones and biomes.

4.4.1. SRZ

For the SRZ, ε_{app} correlates significantly with the amount of precipitation during the growing season (r -0.75, $p < 0.001$), MAP (r -0.75, $p < 0.001$), aridity index (r -0.74, $p < 0.001$), maximum temperature during the warmest month (r 0.72, $p < 0.001$) as well as other environmental factors listed in **Table 3**. There is lower apparent fractionation in more arid regions of the SRZ (**Fig. 7**). This may be caused by several factors. As noted above, D enrichment of soil water due to evaporation affects the isotope composition of leaf waxes and therefore the apparent fractionation between leaf wax and precipitation. Further, the significant correlation with growing season precipitation and MAP suggests that SRZ plants use water immediately after a precipitation event, with a rapid uptake of surface soil water by roots, as well as water from deeper soil layers that incorporate the isotope signature of MAP (Ehleringer and Dawson, 1992; Schulze et al., 1996). Different rooting strategies may influence δD_{wax} composition (Dawson, 1993; Krull et al., 2006; Feakins and Sessions, 2010a; Garcin et al., 2012) leading to lower apparent fractionation in plants with shallower roots than those with deeper roots (Smith and

Freeman, 2006; Berke et al., 2015). However, some studies infer D enrichment of leaf water during leaf transpiration as (the most) important factor that influences apparent fractionation (Smith and Freeman, 2006; Feakins and Sessions, 2010a; Zhou et al., 2011; Kahmen et al., 2013a). In the SRZ of South Africa, D enrichment of leaf water has been previously modelled as ranging between 40‰ in the eastern regions and 70‰ in the drier northwestern parts for the spring season (Kahmen et al., 2013a). The observed ε_{app} range in our soil samples (ca. 50‰) is thus greater than the range for modelled leaf water enrichment (ca. 30‰; Kahmen et al., 2013a). Nevertheless, both values, i.e. ε_{app} of our soil samples and modelled leaf water enrichment, show higher values in the drier western region of the SRZ, indicating that evaporative leaf water enrichment can account for at least part of the detected change in apparent fractionation. Kahmen et al. (2013a) concluded that in arid and temperate environments δD_{wax} records δD composition of precipitation and evapotranspiration, whereas in (wet) tropical environments δD_{wax} records solely δD of precipitation. Our data for the SRZ support this conclusion. The correlation between ε_{app} and the amount of precipitation during the growing season as well as the aridity index (a lower index indicating higher aridity, **Fig. 7**) and annual PET also indicate (Supplementary material Fig. 4) that aridity and therefore evapotranspiration are important in influencing δD_{wax} composition in the SRZ of southern Africa.

In contrast, we find no correlation between ε_{app} and $\delta^{13}C_{wax}$ (**Table 3**) suggesting that the photosynthetic pathway is a negligible factor in influencing ε_{app}. This corroborates previous data, which show that photosynthetic pathway is not a decisive factor controlling hydrogen isotope fractionation in plants (Krull et al., 2006). In contrast,

other studies have shown greater D enrichment in C_4 grasses (dicots) than in C_3 grasses (dicots) (Smith and Freeman, 2006; Liu and Yang, 2008; McInerney et al., 2011; Kahmen et al., 2013b). Additionally, earlier studies have shown a relationship between $\delta^{13}C$ and water use efficiency (WUE) of C_3 plants (e.g. Farquhar et al., 1989; Ehleringer and Dawson, 1992; Rundel et al., 1999). As such, Hou et al. (2007a) inferred that a significant correlation between $\delta^{13}C_{wax}$ and δD_{wax} in tree leaves is related to changing WUE. However, the data from Hou et al. (2007a) are derived solely from tree species within a relatively small area, whereas the vegetation community of plants in southern Africa is a mixture of C_3, C_4 and CAM plants. Whereas $\delta^{13}C_{wax}$ and δD_{wax} were found to correlate negatively for C_3 plants (Bi et al., 2005; Hou et al., 2007a), C_4 and CAM plants showed positive correlations between $\delta^{13}C_{wax}$ and δD_{wax} (Bi et al., 2005; Feakins and Sessions, 2010b) potentially leading to an integrated signal in soils for which there is no correlation between $\delta^{13}C_{wax}$ and δD_{wax} (Supplementary material Fig. 5).

4.4.2. WRZ

In contrast to the SRZ, climatic/environmental parameters are mostly inversely correlated with ε_{app} (**Table 3**). Significant correlations are observed between ε_{app} and the annual range of temperature (r 0.69, $p < 0.001$) and between ε_{app} and the minimum temperature of the coldest quarter (r -0.66, $p < 0.001$) suggesting that temperature conditions affect hydrogen isotope fractionation in this area. Temperature is known to be an important driver for isotopic enrichment in leaf water (Barbour et al., 2000; Zhou et al., 2011; Sachse et al., 2012). As the D composition of soil and plant water remains unknown, we can only assume that the correlation of ε_{app} with temperature is a result of evapotranspiration (e.g. McInerney et al., 2011; Kahmen et al., 2013a, b) or fractionation

during water uptake by plants (e.g. Smith and Freeman, 2006; Feakins and Sessions, 2010a). In the Succulent Karoo biome ε_{app} correlates more strongly with temperature (e.g. MAT: r -0.69, $p < 0.01$) than in the Fynbos biome (MAT: r -0.35, p 0.351), whereas for the latter ε_{app} seems also affected by the PET during the growing season (r 0.87, $p <$ 0.01; **Fig. 8**, **Table 3**).

Additionally, we observe that the seasonal availability of water might affect ε_{app} (r -0.67, $p < 0.001$) in the WRZ. During the drier summer months, an increase in precipitation could reduce drought stress for plants more effectively than a precipitation increase during the wetter winter months (Chase et al., 2015a, b). Reduced drought stress and a greater overall water availability would lead to greater apparent fractionation (Feakins and Sessions, 2010a). Here, however, decreasing precipitation seasonality or increasing precipitation during the dry summer months, which may reduce drought stress, correlate with lower apparent fractionation. This is an unexpected finding. Further, the correlation between precipitation of the dry summer months and ε_{app} only exists for the Succulent Karoo (r 0.77, $p < 0.001$) and not for the Fynbos biome (r 0.36, p 0.344), indicating the possible importance of summer precipitation in the Succulent Karoo.

Differences in the vegetation communities between the Succulent Karoo and Fynbos could be another factor for the observed inverse correlations. In the Karoo, succulents and shrubs develop shallow roots utilizing surface soil water enriched by evaporation (Esler and Rundel, 1999; Shiponeni et al., 2011) including summer precipitation. Most WRZ succulents are CAM plants (Mooney et al., 1977; Boom et al., 2014), which were found to have substantially smaller net apparent fractionation than C_3

or C_4 plants (Feakins and Sessions, 2010b). Succulents produce much higher amounts of wax than, for instance, grasses (Carr et al., 2014; Garcin et al., 2014), which is also reflected in our soil samples (Herrmann et al., 2016). Therefore, δD_{wax} might represent mainly the shallow rooting plants in the Succulent Karoo. In contrast, Fynbos consists of shallow rooted graminoids and shrubs as well as deep rooted shrubs (Hawkins et al., 2009; West et al., 2012).

Despite the dependence of δD_p and ε_{app} on the altitude large topographic changes in the WRZ could cause microclimatic differences between the Succulent Karoo and Fynbos at small spatial scales (Mucina and Rutherford, 2006). This and water uptake by other moisture sources than precipitation as well as different functional plant types between the Succulent Karoo and Fynbos biome may hamper the detection of an obvious relationship between apparent fractionation and environmental parameters. Further investigations are needed to evaluate how δD_p relates to δD_{wax} for the WRZ. Investigations of δD_{wax} from plants and soils along distinct climatic and environmental gradients within the WRZ might solve these questions.

5. Conclusions and palaeoenvironmental implications

We report plant wax δD compositions in soils from various transects in southern Africa comprising a variety of precipitation regimes and vegetation communities. Overall, our study confirms earlier findings using δD_{wax} as a palaeohydrological proxy, and demonstrates that the approach is suitable for climatic reconstruction in southern Africa's SRZ. In semi-arid regions of the SRZ, where the growing season and therefore plant wax production occurs during the warm summer season, the relationship between

525 δD_{wax} and (annual) δD_p as well as MAP suggest that δD_{wax} can be used to reconstruct
526 past precipitation amounts. Evapotranspiration, especially in the more arid parts of the
527 SRZ, lead to isotope enrichment in soil and leaf water and thus less apparent hydrogen
528 isotope fractionation. This effect compromises quantitative precipitation reconstruction.
529 Vegetation changes appear to exert a minor influence on apparent fractionation and
530 δD_{wax} composition. Variations in δD_{wax} in sedimentary archives of the SRZ are thus well-
531 suited for qualitative palaeohydrological reconstruction.

532 In contrast, in the southern African winter rainfall zone, δD_{wax} values do not reflect
533 annual or growing season δD_p. In this area of high topographic variability, distinct
534 microclimatic conditions exist on small spatial scales, likely causing δD_p variation
535 unresolved by the OIPC, but also leading to distinct vegetation communities and
536 vegetation variability as well as potentially differences of additional moisture sources
537 between the biomes in the WRZ. While temperature may be a potential driver for
538 variations in the dry Succulent Karoo biome, potential evapotranspiration seems more
539 important in the Fynbos biome. Further, we detect a potential influence of summer
540 precipitation on the δD_{wax} in the WRZ. Interpretation of past hydrological changes in the
541 WRZ based on δD_{wax} require more care, supported perhaps by a multi proxy approach
542 including pollen, other stable isotopes and/or inorganic geochemical data, as well as a
543 more comprehensive data set for modern plants and soils across the climatic
544 environment of this region. For the WRZ, more research is needed to unravel the factors
545 influencing hydrogen isotope fractionation and δD_{wax}.

546 **Acknowledgements**

This study was funded by the German Bundesministerium für Bildung und Forschung (BMBF) within the project “Regional Archives for Integrated Investigation” (RAiN, 03G0840A). N.H. was supported by GLOMAR – Bremen International Graduate School for Marine Sciences. The work was also supported by the UK Leverhulme Trust (Grant F/00 212/AF) and the European Research Council (ERC) Starting Grant ‘‘HYRAX’’ (Grant Agreement No. 258657). R. Kreutz and O. Helten are thanked for analytical assistance and T. Eickhorst for help with soil import. We thank the editors for their time and valuable remarks and the two anonymous reviewers for their constructive comments.

References

Aichner, B., Herzschuh, U., Wilkes, H., Vieth, A., Böhner, J., 2010. δD values of *n*-alkanes in Tibetan lake sediments and aquatic macrophytes – A surface sediment study and application to a 16ka record from Lake Koucha. Organic Geochemistry 41, 779–790. doi:10.1016/j.orggeochem.2010.05.010

Araguás-Araguás, L., Froehlich, K., Rozanski, K., 2000. Deuterium and ^{18}O isotope composition of precipitation and atmospheric moisture. Hydrological Processes 14, 1341–1355. doi:10.1002/1099-1085(20000615)14:8<1341::AID-HYP983>3.0.CO;2-Z

Barbour, M.M., Fischer, R.A., Sayre, K.D., Farquhar, G.D., 2000. Oxygen isotope ratio of leaf and grain material correlates with stomatal conductance and grain yield in irrigated wheat. Functional Plant Biology 27, 625–637.

Berke, M.A., Tipple, B.J., Hambach, B., Ehleringer, J.R., 2015. Life form-specific gradients in compound-specific hydrogen isotope ratios of modern leaf waxes along a North American Monsoonal transect. Oecologia 179, 981–97. doi:10.1007/s00442-015-3432-1

Bi, X., Sheng, G., Liu, X., Li, C., Fu, J., 2005. Molecular and carbon and hydrogen isotopic composition of *n*-alkanes in plant leaf waxes. Organic Geochemistry 36, 1405–1417. doi:10.1016/j.orggeochem.2005.06.001

Boom, A., Carr, A.S., Chase, B.M., Grimes, H.L., Meadows, M.E., 2014. Leaf wax *n*-alkanes and $\delta^{13}C$ values of CAM plants from arid southwest Africa. Organic Geochemistry 67, 99–102. doi:10.1016/j.orggeochem.2013.12.005

Bowen, G.J., Revenaugh, J., 2003. Interpolating the isotopic composition of modern meteoric precipitation. Water Resources Research 39, 1299.

Bowen, G.J., Wassenaar, L.I., Hobson, K.A., 2005. Global application of stable hydrogen and oxygen isotopes to wildlife forensics. Oecologia 143, 337–48. doi:10.1007/s00442-004-1813-y

Bush, R.T., McInerney, F.A., 2013. Leaf wax *n*-alkane distributions in and across modern plants: Implications for paleoecology and chemotaxonomy. Geochimica et Cosmochimica Acta 117, 161–179. doi:10.1016/j.gca.2013.04.016

Carr, A.S., Boom, A., Chase, B.M., Meadows, M.E., Roberts, Z.E., Britton, M.N., Cumming, A.M.J., 2013. Biome-scale characterisation and differentiation of semi-arid and arid zone soil organic matter compositions using pyrolysis–GC/MS analysis. Geoderma 200–201, 189–201. doi:10.1016/j.geoderma.2013.02.012

Carr, A.S., Boom, A., Grimes, H.L., Chase, B.M., Meadows, M.E., Harris, A., 2014. Leaf wax *n*-alkane distributions in arid zone South African flora: Environmental controls, chemotaxonomy and palaeoecological implications. Organic Geochemistry 67, 72–84. doi:10.1016/j.orggeochem.2013.12.004

Chase, B.M., Boom, A., Carr, A.S., Carré, M., Chevalier, M., Meadows, M.E., Pedro, J.B., Stager, J.C., Reimer, P.J., 2015a. Evolving southwest African response to abrupt deglacial North Atlantic climate change events. Quaternary Science Reviews 121, 132–136. doi:10.1016/j.quascirev.2015.05.023

598 Chase, B.M., Lim, S., Chevalier, M., Boom, A., Carr, A.S., Meadows, M.E., Reimer, P.J.,
599 2015b. Influence of tropical easterlies in southern Africa's winter rainfall zone during
600 the Holocene. Quaternary Science Reviews 107, 138–148.
601 doi:10.1016/j.quascirev.2014.10.011

602 Chase, B.M., Meadows, M.E., 2007. Late Quaternary dynamics of southern Africa's
603 winter rainfall zone. Earth-Science Reviews 84, 103–138.
604 doi:10.1016/j.earscirev.2007.06.002

605 Chikaraishi, Y., Naraoka, H., 2006. Carbon and hydrogen isotope variation of plant
606 biomarkers in a plant–soil system. Chemical Geology 231, 190–202.
607 doi:10.1016/j.chemgeo.2006.01.026

608 Collins, J.A., Schefuß, E., Mulitza, S., Prange, M., Werner, M., Tharammal, T., Paul, A.,
609 Wefer, G., 2013. Estimating the hydrogen isotopic composition of past precipitation
610 using leaf-waxes from western Africa. Quaternary Science Reviews 65, 88–101.

611 Cowling, R.M., Richardson, D.M., Pierce, S.M., 1997. Vegetation of Southern Africa.
612 Cambridge University Press.

613 Dansgaard, W., 1964. Stable isotopes in precipitation. Tellus 16, 436–468.
614 doi:10.1111/j.2153-3490.1964.tb00181.x

615 Dawson, T.E., 1993. Hydraulic lift and water use by plants: implications for water
616 balance, performance and plant-plant interactions. Oecologia 95, 565–574.
617 doi:10.1007/BF00317442

618 de Vries, J.J., Selaolo, E.T., Beekman, H.E., 2000. Groundwater recharge in the
619 Kalahari, with reference to paleo-hydrologic conditions. Journal of Hydrology 238,
620 110–123. doi:10.1016/S0022-1694(00)00325-5

621 Diamond, R.E., 2014. Stable isotope hydrology of the Table Mountain group (PhD
622 thesis). University of Cape Town.

623 Diefendorf, A.F., Freeman, K.H., Wing, S.L., Graham, H. V., 2011. Production of *n*-alkyl
624 lipids in living plants and implications for the geologic past. Geochimica et
625 Cosmochimica Acta 75, 7472–7485. doi:10.1016/j.gca.2011.09.028

626 Douglas, P.M.J., Pagani, M., Brenner, M., Hodell, D.A., Curtis, J.H., 2012. Aridity and
627 vegetation composition are important determinants of leaf-wax δD values in
628 southeastern Mexico and Central America. Geochimica et Cosmochimica Acta 97,
629 24–45. doi:10.1016/j.gca.2012.09.005

630 Dupont, L., Wyputta, U., 2003. Reconstructing pathways of aeolian pollen transport to
631 the marine sediments along the coastline of SW Africa. Quaternary Science
632 Reviews 22, 157–174. doi:10.1016/S0277-3791(02)00032-X

633 Eckardt, F.D., Kuring, N., 2005. SeaWiFS identifies dust sources in the Namib Desert.
634 International Journal of Remote Sensing 26, 4159–4167.
635 doi:10.1080/01431160500113112

636 Eglinton, T.I., Eglinton, G., 2008. Molecular proxies for paleoclimatology. Earth and
637 Planetary Science Letters 275, 1–16. doi:10.1016/j.epsl.2008.07.012

638 Ehleringer, J.R., Dawson, T.E., 1992. Water uptake by plants: perspectives from stable
639 isotope composition. Plant, Cell and Environment 15, 1073–1082.

doi:10.1111/j.1365-3040.1992.tb01657.x

Esler, K.J., Rundel, P.W., 1999. Comparative Patterns of Phenology and Growth Form Diversity in Two Winter Rainfall Deserts: The Succulent Karoo and Mojave Desert Ecosystems. Plant Ecology 142, 97–104.

Farquhar, G.D., Ehleringer, J.R., Hubick, K.T., 1989. Carbon Isotope Discrimination and Photosynthesis. Annual Review of Plant Physiology and Plant Molecular Biology 40, 503–537. doi:10.1146/annurev.pp.40.060189.002443

Feakins, S.J., Bentley, L.P., Salinas, N., Shenkin, A., Blonder, B., Goldsmith, G.R., Ponton, C., Arvin, L.J., Wu, M.S., Peters, T., West, A.J., Martin, R.E., Enquist, B.J., Asner, G.P., Malhi, Y., 2016. Plant leaf wax biomarkers capture gradients in hydrogen isotopes of precipitation from the Andes and Amazon. Geochimica et Cosmochimica Acta 182, 155–172. doi:10.1016/j.gca.2016.03.018

Feakins, S.J., Sessions, A.L., 2010a. Controls on the D/H ratios of plant leaf waxes in an arid ecosystem. Geochimica et Cosmochimica Acta 74, 2128–2141. doi:10.1016/j.gca.2010.01.016

Feakins, S.J., Sessions, A.L., 2010b. Crassulacean acid metabolism influences D/H ratio of leaf wax in succulent plants. Organic Geochemistry 41, 1269–1276.

Flanagan, L.B., Ehleringer, J.R., 1991. Stable Isotope Composition of Stem and Leaf Water: Applications to the Study of Plant Water Use. Functional Ecology 5, 270–277. doi:10.2307/2389264

Gamarra, B., Sachse, D., Kahmen, A., 2016. Effects of leaf water evaporative ^{2}H-enrichment and biosynthetic fractionation on leaf wax *n*-alkane $\delta^{2}H$ values in C3 and C4 grasses. Plant, Cell & Environment. doi:10.1111/pce.12789

Gao, L., Edwards, E.J., Zeng, Y., Huang, Y., 2014. Major evolutionary trends in hydrogen isotope fractionation of vascular plant leaf waxes. PloS ONE 9, e112610. doi:10.1371/journal.pone.0112610

Gao, L., Guimond, J., Thomas, E., Huang, Y., 2015. Major trends in leaf wax abundance, $\delta^{2}H$ and $\delta^{13}C$ values along leaf venation in five species of C_3 plants: Physiological and geochemical implications. Organic Geochemistry 78, 144–152. doi:10.1016/j.orggeochem.2014.11.005

Garcin, Y., Schefuß, E., Schwab, V.F., Garreta, V., Gleixner, G., Vincens, A., Todou, G., Séné, O., Onana, J.-M., Achoundong, G., Sachse, D., 2014. Reconstructing C_3 and C_4 vegetation cover using *n*-alkane carbon isotope ratios in recent lake sediments from Cameroon, Western Central Africa. Geochimica et Cosmochimica Acta 142, 482–500. doi:10.1016/j.gca.2014.07.004

Garcin, Y., Schwab, V.F., Gleixner, G., Kahmen, A., Todou, G., Séné, O., Onana, J.-M., Achoundong, G., Sachse, D., 2012. Hydrogen isotope ratios of lacustrine sedimentary *n*-alkanes as proxies of tropical African hydrology: Insights from a calibration transect across Cameroon. Geochimica et Cosmochimica Acta 79, 106–126. doi:10.1016/j.gca.2011.11.039

Gat, J.R., 1996. Oxygen and hydrogen isotopes in the hydrologic cycle. Annual Review of Earth and Planetary Sciences 24, 225–262. doi:10.1146/annurev.earth.24.1.225

682 Harris, C., Burgers, C., Miller, J., Rawoot, F., 2010. O- and H-isotope record of Cape
683 Town rainfall from 1996 to 2008, and its application to recharge studies of Table
684 Mountain groundwater, South Africa. South African Journal of Geology 113, 33–56.
685 doi:10.2113/gssajg.113.1.33

686 Hawkins, H., Hettasch, H., West, A.G., Cramer, M.D., 2009. Hydraulic redistribution by
687 Protea “Sylvia” (Proteaceae) facilitates soil water replenishment and water
688 acquisition by an understorey grass and shrub. Functional Plant Biology 36, 752–
689 760.

690 Herrmann, N., Boom, A., Carr, A.S., Chase, B.M., Granger, R., Hahn, A., Zabel, M.,
691 Schefuß, E., 2016. Sources, transport and deposition of terrestrial organic material:
692 A case study from southwestern Africa. Quaternary Science Reviews 149, 215–229.
693 doi:10.1016/j.quascirev.2016.07.028

694 Hijmans, R.J., Cameron, S.E., Parra, J.L., Jones, P.G., Jarvis, A., 2005. Very high
695 resolution interpolated climate surfaces for global land areas. International Journal
696 of Climatology 25, 1965–1978. doi:10.1002/joc.1276

697 Holdsworth, G., Fogarasi, S., Krouse, H.R., 1991. Variation of the stable isotopes of
698 water with altitude in the Saint Elias Mountains of Canada. Journal of Geophysical
699 Research 96, 7483–7494. doi:10.1029/91JD00048

700 Hou, J., D’Andrea, W.J., Huang, Y., 2008. Can sedimentary leaf waxes record D/H ratios
701 of continental precipitation? Field, model, and experimental assessments.
702 Geochimica et Cosmochimica Acta 72, 3503–3517. doi:10.1016/j.gca.2008.04.030

703 Hou, J., D’Andrea, W.J., MacDonald, D., Huang, Y., 2007a. Evidence for water use
704 efficiency as an important factor in determining the δD values of tree leaf waxes.
705 Organic Geochemistry 38, 1251–1255. doi:10.1016/j.orggeochem.2007.03.011

706 Hou, J., D’Andrea, W.J., MacDonald, D., Huang, Y., 2007b. Hydrogen isotopic variability
707 in leaf waxes among terrestrial and aquatic plants around Blood Pond,
708 Massachusetts (USA). Organic Geochemistry 38, 977–984.
709 doi:10.1016/j.orggeochem.2006.12.009

710 Houze, R.A., 2012. Orographic effects on precipitating clouds. Reviews of Geophysics
711 50, RG1001. doi:10.1029/2011RG000365

712 Jia, G., Wei, K., Chen, F., Peng, P., 2008. Soil *n*-alkane δD vs. altitude gradients along
713 Mount Gongga, China. Geochimica et Cosmochimica Acta 72, 5165–5174.
714 doi:10.1016/j.gca.2008.08.004

715 Kahmen, A., Hoffmann, B., Schefuß, E., Arndt, S.K., Cernusak, L.A., West, J.B.,
716 Sachse, D., 2013a. Leaf water deuterium enrichment shapes leaf wax *n*-alkane δD
717 values of angiosperm plants II: Observational evidence and global implications.
718 Geochimica et Cosmochimica Acta 111, 50–63. doi:10.1016/j.gca.2012.09.004

719 Kahmen, A., Schefuß, E., Sachse, D., 2013b. Leaf water deuterium enrichment shapes
720 leaf wax *n*-alkane δD values of angiosperm plants I: Experimental evidence and
721 mechanistic insights. Geochimica et Cosmochimica Acta 111, 39–49.
722 doi:10.1016/j.gca.2012.09.003

723 Kortelainen, N.M., Karhu, J.A., 2004. Regional and seasonal trends in the oxygen and

hydrogen isotope ratios of Finnish groundwaters: a key for mean annual precipitation. Journal of Hydrology 285, 143–157. doi:10.1016/j.jhydrol.2003.08.014

Krull, E., Sachse, D., Mügler, I., Thiele, A., Gleixner, G., 2006. Compound-specific $\delta^{13}C$ and $\delta^{2}H$ analyses of plant and soil organic matter: A preliminary assessment of the effects of vegetation change on ecosystem hydrology. Soil Biology and Biochemistry 38, 3211–3221. doi:10.1016/j.soilbio.2006.04.008

Kuechler, R.R., Schefuß, E., Beckmann, B., Dupont, L., Wefer, G., 2013. NW African hydrology and vegetation during the Last Glacial cycle reflected in plant-wax-specific hydrogen and carbon isotopes. Quaternary Science Reviews 82, 56–67. doi:10.1016/j.quascirev.2013.10.013

Liu, W., Yang, H., 2008. Multiple controls for the variability of hydrogen isotopic compositions in higher plant *n*-alkanes from modern ecosystems. Global Change Biology 14, 2166–2177. doi:10.1111/j.1365-2486.2008.01608.x

Liu, W., Yang, H., Li, L., 2006. Hydrogen isotopic compositions of *n*-alkanes from terrestrial plants correlate with their ecological life forms. Oecologia 150, 330–338. doi:10.1007/s00442-006-0494-0

Luo, P., Peng, P., Gleixner, G., Zheng, Z., Pang, Z., Ding, Z., 2011. Empirical relationship between leaf wax *n*-alkane δD and altitude in the Wuyi, Shennongjia and Tianshan Mountains, China: Implications for paleoaltimetry. Earth and Planetary Science Letters 301, 285–296. doi:10.1016/j.epsl.2010.11.012

Matimati, I., Musil, C.F., Raitt, L., February, E., 2013. Non rainfall moisture interception by dwarf succulents and their relative abundance in an inland arid South African ecosystem. Ecohydrology 6, 818–825. doi:10.1002/eco.1304

McInerney, F.A., Helliker, B.R., Freeman, K.H., 2011. Hydrogen isotope ratios of leaf wax *n*-alkanes in grasses are insensitive to transpiration. Geochimica et Cosmochimica Acta 75, 541–554. doi:10.1016/j.gca.2010.10.022

Mooney, H.A., Troughton, J.H., Berry, J.A., 1977. Carbon isotope ratio measurements of succulent plants in southern Africa. Oecologia 30, 295–305. doi:10.1007/BF00399762

Mucina, L., Rutherford, M., 2006. The vegetation of South Africa, Lesotho and Swaziland., in: The Vegetation of South Africa Lesotho and Sawziland. pp. 749–790. doi:10.1007/s

Musekiwa, C., Majola, K., 2013. Groundwater vulnerability Map for south africa. South African Journal of Geomatics 2, 152–162.

Niedermeyer, E.M., Forrest, M., Beckmann, B., Sessions, A.L., Mulch, A., Schefuß, E., 2016. The stable hydrogen isotopic composition of sedimentary plant waxes as quantitative proxy for rainfall in the West African Sahel. Geochimica et Cosmochimica Acta 184, 55–70. doi:10.1016/j.gca.2016.03.034

Niedermeyer, E.M., Schefuß, E., Sessions, A.L., Mulitza, S., Mollenhauer, G., Schulz, M., Wefer, G., 2010. Orbital- and millennial-scale changes in the hydrologic cycle and vegetation in the western African Sahel: insights from individual plant wax δD and $\delta^{13}C$. Quaternary Science Reviews 29, 2996–3005.

doi:10.1016/j.quascirev.2010.06.039

Polissar, P.J., Freeman, K.H., 2010. Effects of aridity and vegetation on plant-wax δD in modern lake sediments. Geochimica et Cosmochimica Acta 74, 5785–5797. doi:10.1016/j.gca.2010.06.018

Prospero, J.M., Ginoux, P., Torres, O., Nicholson, S.E., Gill, T.E., 2002. Environmental characterization of global sources of atmospheric soil dust identified with the NIMBUS 7 Total Ozone Mapping Spectrometer (TOMS) absorbing aerosol product. Reviews of Geophysics 40, 1002. doi:10.1029/2000RG000095

Rao, Z., Zhu, Z., Jia, G., Henderson, A.C.G., Xue, Q., Wang, S., 2009. Compound specific δD values of long chain *n*-alkanes derived from terrestrial higher plants are indicative of the δD of meteoric waters: Evidence from surface soils in eastern China. Organic Geochemistry 40, 922–930. doi:10.1016/j.orggeochem.2009.04.011

Risi, C., Bony, S., Vimeux, F., 2008. Influence of convective processes on the isotopic composition ($\delta^{18}O$ and δD) of precipitation and water vapor in the tropics: 2. Physical interpretation of the amount effect. Journal of Geophysical Research Atmospheres 113. doi:10.1029/2008JD009943

Rozanski, K., 1985. Deuterium and ^{18}O in European groundwaters — Links to atmospheric circulation in the past. Chemical Geology: Isotope Geoscience section 52, 349–363. doi:10.1016/0168-9622(85)90045-4

Rozanski, K., Araguás-Araguás, L., Gonfiantini, R., 1993. Isotopic Patterns in Modern Global Precipitation. Climate Change in Continental Isotopic Records 78, 1–36. doi:10.1029/GM078p0001

Rundel, P.W., Dillon, M.O., Palma, B., Mooney, H.A., Gulmon, S.L., Ehleringer, J.R., 1991. The phytogeography and ecology of the coastal Atacama and Peruvian deserts. Aliso.

Rundel, P.W., Esler, K.J., Cowling, R.M., 1999. Ecological and Phylogenetic Patterns of Carbon Isotope Discrimination in the Winter-Rainfall Flora of the Richtersveld, South Africa. Plant Ecology 142, 133–148.

Sachse, D., Billault, I., Bowen, G.J., Chikaraishi, Y., Dawson, T.E., Feakins, S.J., Freeman, K.H., Magill, C.R., McInerney, F. a., van der Meer, M.T.J., Polissar, P., Robins, R.J., Sachs, J.P., Schmidt, H.-L., Sessions, A.L., White, J.W.C., West, J.B., Kahmen, A., 2012. Molecular Paleohydrology: Interpreting the Hydrogen-Isotopic Composition of Lipid Biomarkers from Photosynthesizing Organisms. Annual Review of Earth and Planetary Sciences 40, 221–249. doi:10.1146/annurev-earth-042711-105535

Sachse, D., Radke, J., Gleixner, G., 2006. δD values of individual *n*-alkanes from terrestrial plants along a climatic gradient – Implications for the sedimentary biomarker record. Organic Geochemistry 37, 469–483. doi:10.1016/j.orggeochem.2005.12.003

Sachse, D., Radke, J., Gleixner, G., 2004. Hydrogen isotope ratios of recent lacustrine sedimentary *n*-alkanes record modern climate variability. Geochimica et Cosmochimica Acta 68, 4877–4889. doi:10.1016/j.gca.2004.06.004

Schefuß, E., Schouten, S., Schneider, R.R., 2005. Climatic controls on central African hydrology during the past 20,000 years. Nature 437, 1003–1006.

Schimmelmann, A., Sessions, A.L., Mastalerz, M., 2006. Hydrogen isotopic (D/H) composition of organic matter during diagenesis and thermal maturation. Annual Review of Earth and Planetary Sciences 34, 501–533. doi:10.1146/annurev.earth.34.031405.125011

Schulze, E.-D., Mooney, H.A., Sala, O.E., Jobbagy, E., Buchmann, N., Bauer, G., Canadell, J., Jackson, R.B., Loreti, J., Oesterheld, M., Ehleringer, J.R., 1996. Rooting depth, water availability, and vegetation cover along an aridity gradient in Patagonia. Oecologia 108, 503–511. doi:10.1007/BF00333727

Schwab, V.F., Garcin, Y., Sachse, D., Todou, G., Séné, O., Onana, J.-M., Achoundong, G., Gleixner, G., 2015. Effect of aridity on $\delta^{13}C$ and δD values of C_3 plant- and C_4 graminoid-derived leaf wax lipids from soils along an environmental gradient in Cameroon (Western Central Africa). Organic Geochemistry 78, 99–109. doi:10.1016/j.orggeochem.2014.09.007

Scott, L., Neumann, F.H., Brook, G.A., Bousman, C.B., Norström, E., Metwally, A.A., 2012. Terrestrial fossil-pollen evidence of climate change during the last 26 thousand years in Southern Africa. Quaternary Science Reviews 32, 100–118. doi:10.1016/j.quascirev.2011.11.010

Scott, L., Vogel, J.C., 2000. Evidence for environmental conditions during the last 20000 years in Southern Africa from 13C in fossil hyrax dung. Global and Planetary Change 26, 207–215.

Seki, O., Meyers, P.A., Kawamura, K., Zheng, Y., Zhou, W., 2009. Hydrogen isotopic ratios of plant wax *n*-alkanes in a peat bog deposited in northeast China during the last 16kyr. Organic Geochemistry 40, 671–677. doi:10.1016/j.orggeochem.2009.03.007

Seki, O., Nakatsuka, T., Shibata, H., Kawamura, K., 2010. A compound-specific *n*-alkane $\delta^{13}C$ and δD approach for assessing source and delivery processes of terrestrial organic matter within a forested watershed in northern Japan. Geochimica et Cosmochimica Acta 74, 599–613. doi:10.1016/j.gca.2009.10.025

Shiponeni, N., Allsopp, N., Carrick, P.J., Hoffman, M.T., 2011. Competitive interactions between grass and succulent shrubs at the ecotone between an arid grassland and succulent shrubland in the Karoo. Plant Ecology 212, 795–808. doi:10.1007/s11258-010-9864-0

Smith, F.A., Freeman, K.H., 2006. Influence of physiology and climate on δD of leaf wax *n*-alkanes from C_3 and C_4 grasses. Geochimica et Cosmochimica Acta 70, 1172–1187. doi:10.1016/j.gca.2005.11.006

Soderberg, K.S., 2010. The role of fog in the ecohydrology and biogeochemistry of the Namib Desert.

Still, C.J., Powell, R.L., 2010. Continental-scale distributions of vegetation stable carbon isotope ratios, in: Isoscapes: Understanding Movement, Pattern, and Process on Earth through Isotope Mapping. pp. 179–193. doi:10.1007/978-90-481-3354-3_9

Ting, I.P., 1985. Crassulacean acid metabolism. Annual Review of Plant Physiology 36, 595–622.

Trabucco, A., Zomer, R.J., 2009. Global Aridity Index (Global-Aridity) and Global Potential Evapo-Transpiration (Global-PET) Geospatial Database. CGIAR Consortium for Spatial Information. Published online, available from the CGIAR-CSI GeoPortal at: http://www.csi.cgiar.org/.

Tuthorn, M., Zech, R., Ruppenthal, M., Oelmann, Y., Kahmen, A., del Valle, H.F., Eglinton, T., Rozanski, K., Zech, M., 2015. Coupling δ^2H and $\delta^{18}O$ biomarker results yields information on relative humidity and isotopic composition of precipitation – a climate transect validation study. Biogeosciences 12, 3913–3924. doi:10.5194/bg-12-3913-2015

Tyson, P.D., 1986. Climatic change and variability in southern Africa. Oxford University Press, Cape Town ; New York.

Tyson, P.D., Preston-Whyte, R.A., 2000. The Weather and Climate of Southern Africa. Oxford University Press Southern Africa.

Vickery, K.J., Eckardt, F.D., Bryant, R.G., 2013. A sub-basin scale dust plume source frequency inventory for southern Africa, 2005–2008. Geophysical Research Letters 40, 5274–5279.

Vogel, J.C., 1978. Recycling of carbon in a forest environment. Oecologia Plantarum 13, 89–94.

Wassenaar, L.I., Van Wilgenburg, S.L., Larson, K., Hobson, K.A., 2009. A groundwater isoscape (δD, $\delta^{18}O$) for Mexico. Journal of Geochemical Exploration 102, 123–136. doi:10.1016/j.gexplo.2009.01.001

Werger, M.J.A., Ellis, R.P., 1981. Photosynthetic pathways in the arid regions of South Africa. Flora 171, 64–75.

West, A.G., Dawson, T.E., February, E.C., Midgley, G.F., Bond, W.J., Aston, T.L., 2012. Diverse functional responses to drought in a Mediterranean-type shrubland in South Africa. New Phytologist 195, 396–407. doi:10.1111/j.1469-8137.2012.04170.x

West, A.G., February, E.C., Bowen, G.J., 2014. Spatial analysis of hydrogen and oxygen stable isotopes ("isoscapes") in ground water and tap water across South Africa. Journal of Geochemical Exploration 145, 213–222. doi:10.1016/j.gexplo.2014.06.009

Worden, J., Noone, D., Bowman, K., 2007. Importance of rain evaporation and continental convection in the tropical water cycle. Nature 445, 528–32. doi:10.1038/nature05508

Zech, M., Zech, R., Rozanski, K., Gleixner, G., Zech, W., 2015. Do *n*-alkane biomarkers in soils/sediments reflect the δ^2H isotopic composition of precipitation? A case study from Mt. Kilimanjaro and implications for paleoaltimetry and paleoclimate research. Isotopes in Environmental and Health Studies 1–17. doi:10.1080/10256016.2015.1058790

Zhou, Y., Grice, K., Chikaraishi, Y., Stuart-Williams, H., Farquhar, G.D., Ohkouchi, N., 2011. Temperature effect on leaf water deuterium enrichment and isotopic

892 fractionation during leaf lipid biosynthesis: Results from controlled growth of C_3 and
893 C_4 land plants. Phytochemistry 72, 207–213. doi:10.1016/j.phytochem.2010.10.022

894

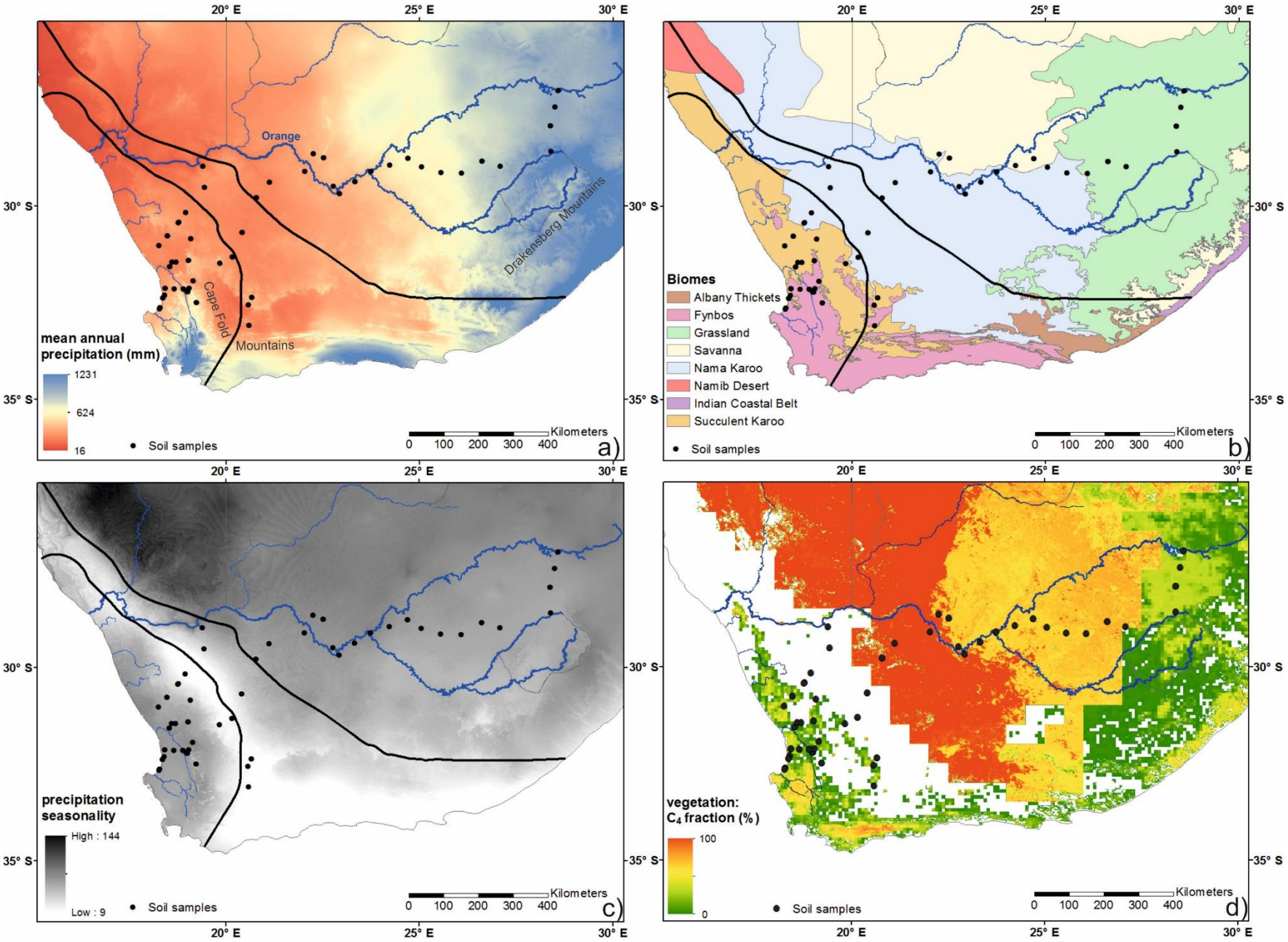

Fig. 1. Study area in southern Africa showing (a) mean annual precipitation and (b) modern biome distribution (after Mucina and Rutherford, 2006; Scott et al., 2012), (c) precipitation seasonality obtained from WorldClim 1.4 Global Climate data (1960-1990 avg.) at 1 km² resolution (Hijmans et al., 2005) and (d) C_4 vegetation coverage from remote sensing and modelled data; white areas have minimal vegetation coverage (Still and Powell, 2010). Boundaries of the different main rainfall zones are indicated with black lines and locations of the soil samples with black dots.

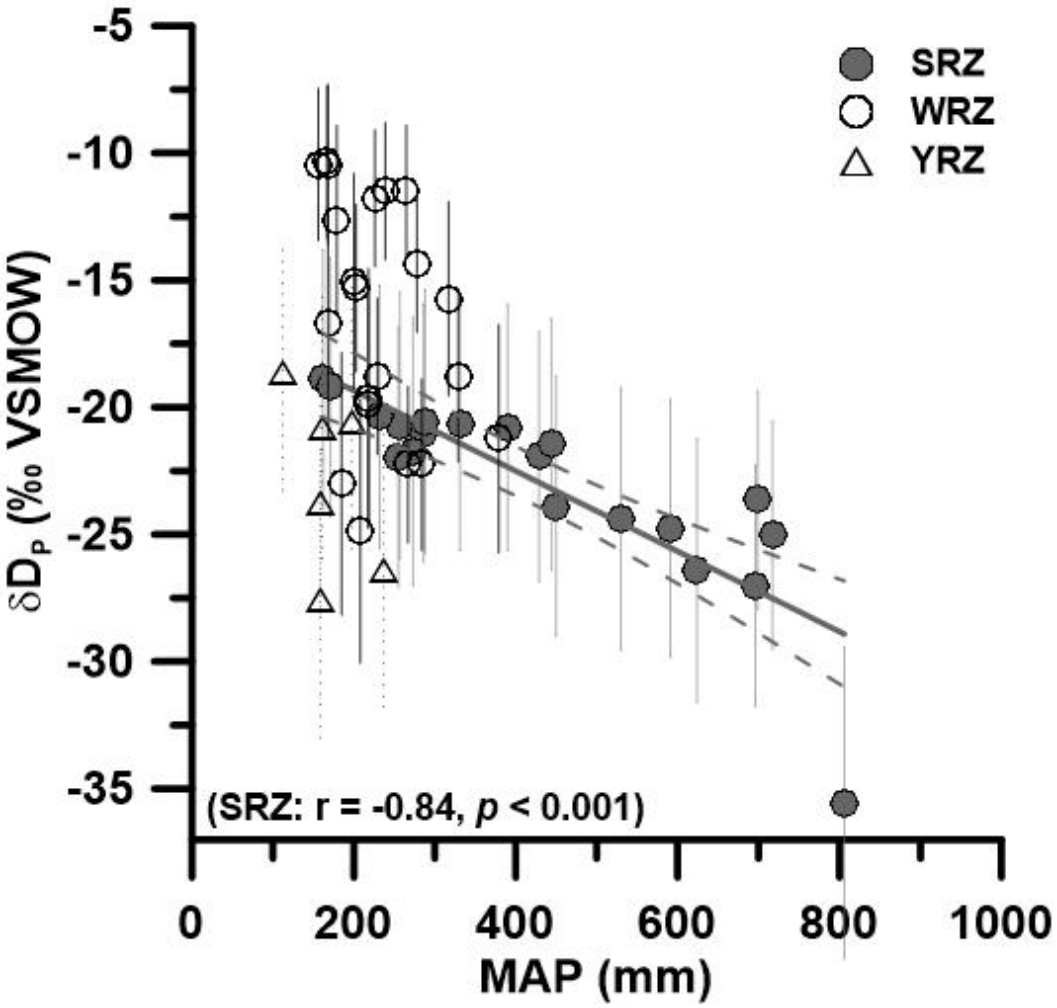

Fig. 2. Comparison of mean annual precipitation (MAP; Hijmans et al., 2005) and interpolated δD values of annual precipitation (OIPC; Bowen and Revenaugh, 2003) for the locations in the study area. The locations are divided into the summer rainfall (SRZ, closed grey dots), winter rainfall (WRZ, open dots) and year round rainfall (YRZ, open triangles) zones. Grey line indicates the linear fit for the SRZ data and dashed lines indicate the 95% confidence interval.

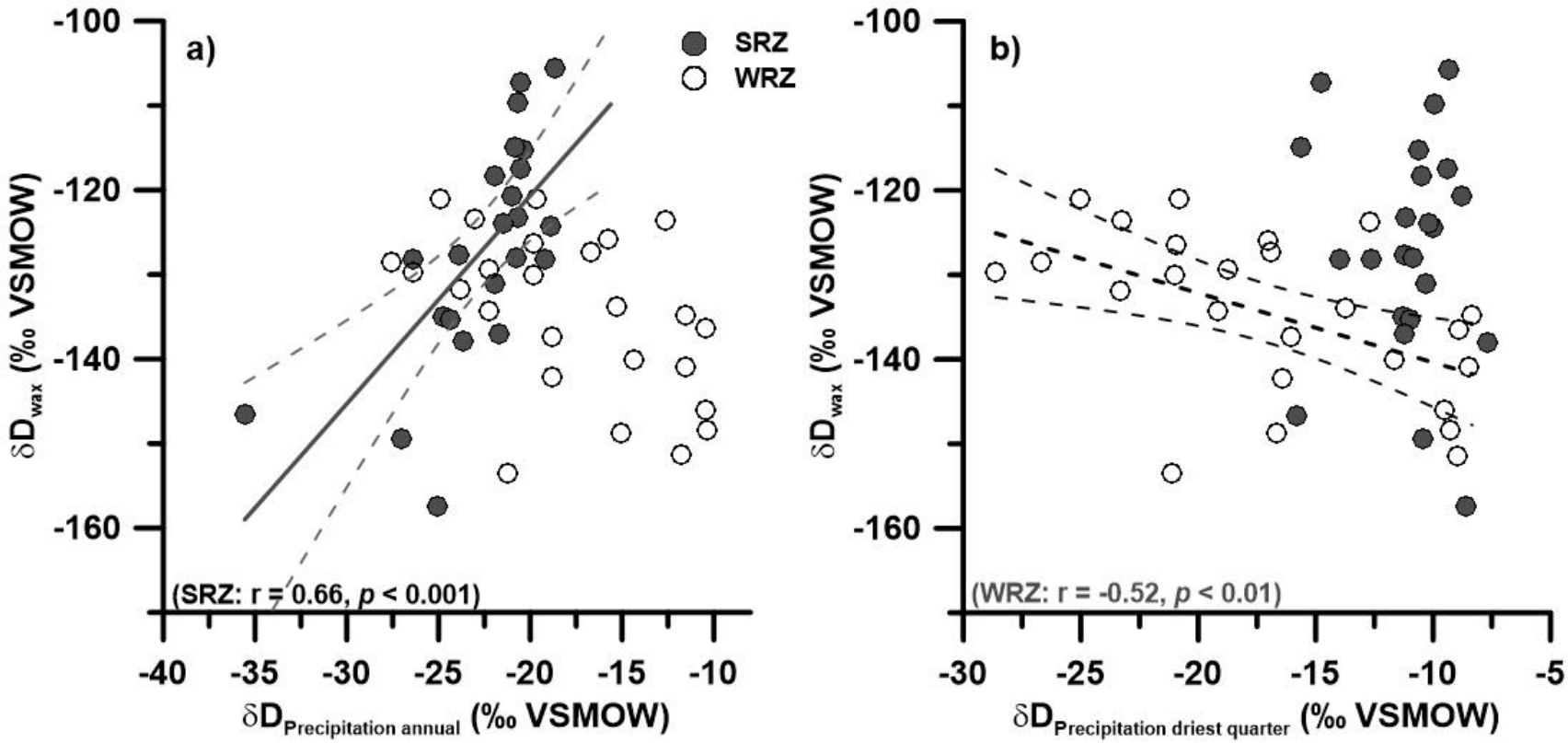

903

904 **Fig. 3.**Comparison of compound-specific δD_{wax} (amount weighted mean of C_{29} and C_{31}) and δD of annual precipitation (left) as well as δD_{wax} and δD of

905 the driest quarter (right) for the soil samples. The locations of the soils are divided into summer rainfall (SRZ, closed grey dots) and winter rainfall

906 (WRZ, open dots) zones in (a,b). The grey line in a) line shows the linear fit in the SRZ and the black dashed line in b) shows the linear fit in the WRZ.

907 Dashed lines around the linear fits indicate the 95% confidence interval. Isotope data for precipitation are from OIPC (Bowen and Revenaugh, 2003).

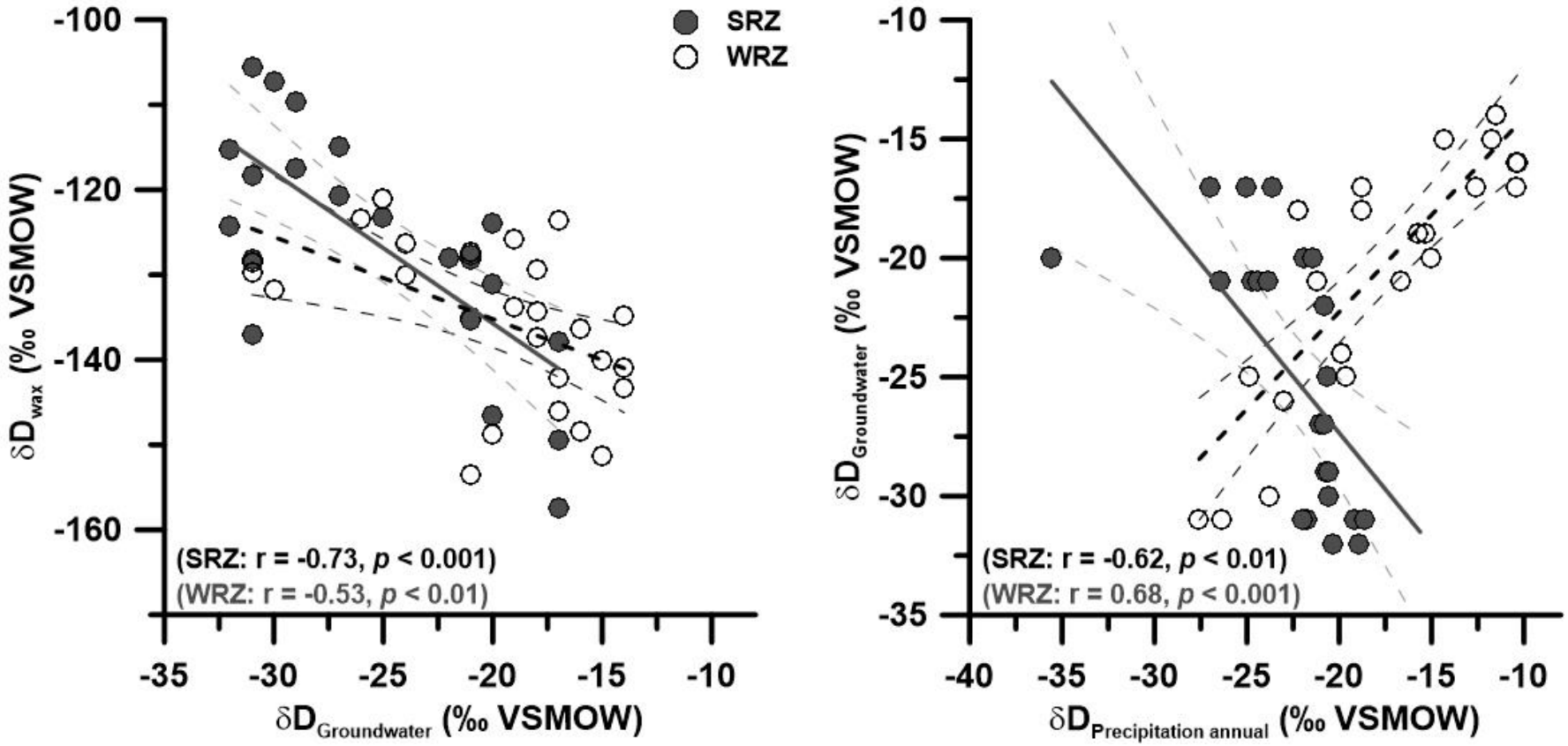

908

909 **Fig. 4.** Comparison of compound-specific δD_{wax} (amount weighted mean of C_{29} and C_{31}) and interpolated δD of groundwater (left, West et al., 2014) as

910 well as δD values of groundwater and annual precipitation (right, Bowen and Revenaugh, 2003) for the locations of the soil samples. The locations are

911 divided into summer rainfall (SRZ, closed grey dots) and winter rainfall zones (WRZ, open dots). Linear fits and 95% confidence intervals are shown

912 for both rainfall zones. Thick grey lines are the linear fits for the SRZ and thick dashed lines are the linear fits for the WRZ.

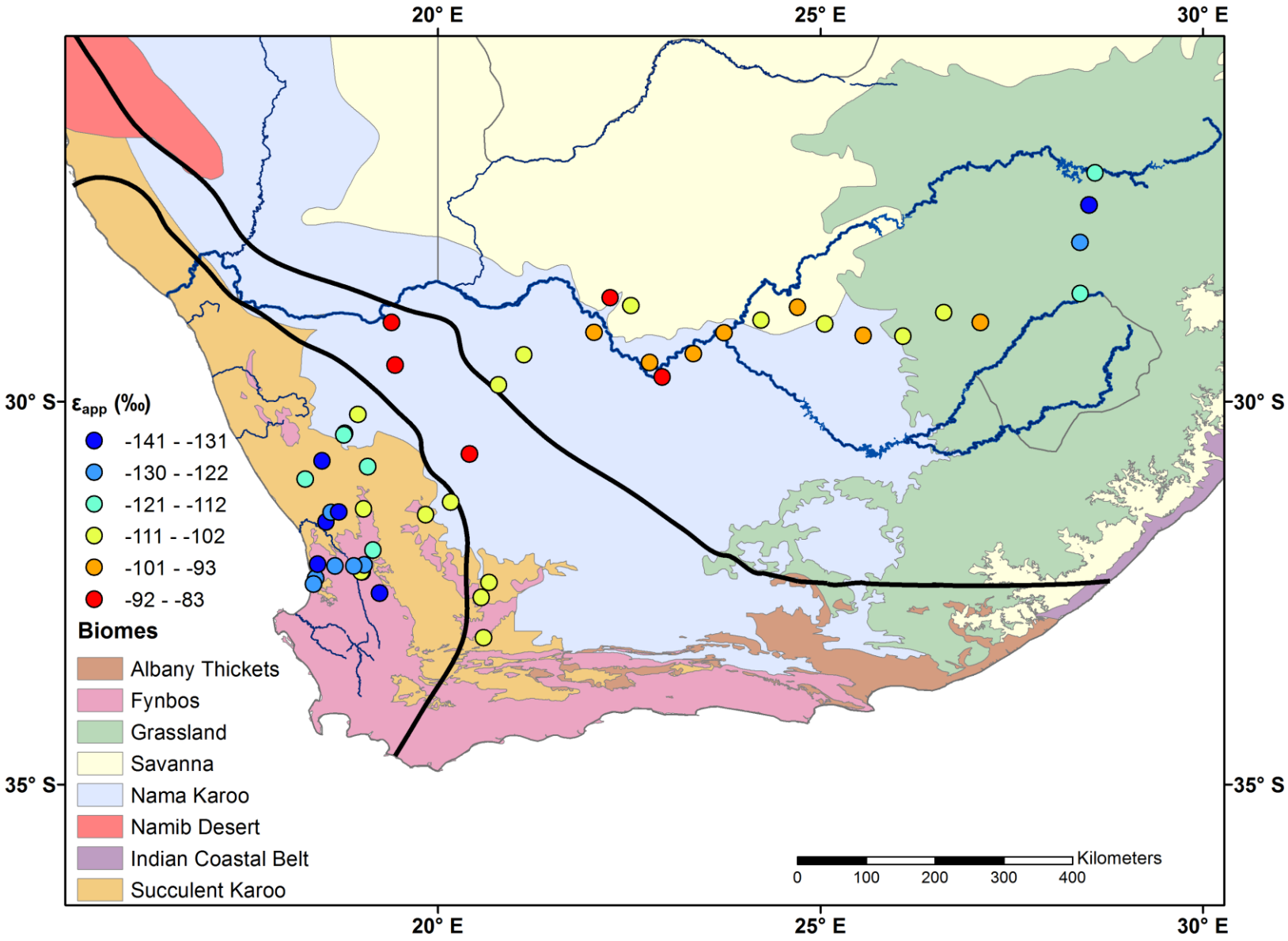

913 Fig. 5. Amount weighted mean apparent hydrogen isotope fractionation (ε_{app}) values of plant wax alkanes in the study area with

914 modern biomes (after Mucina and Rutherford, 2006; Scott et al., 2012). Boundaries of the main rainfall zones are indicated with black lines.

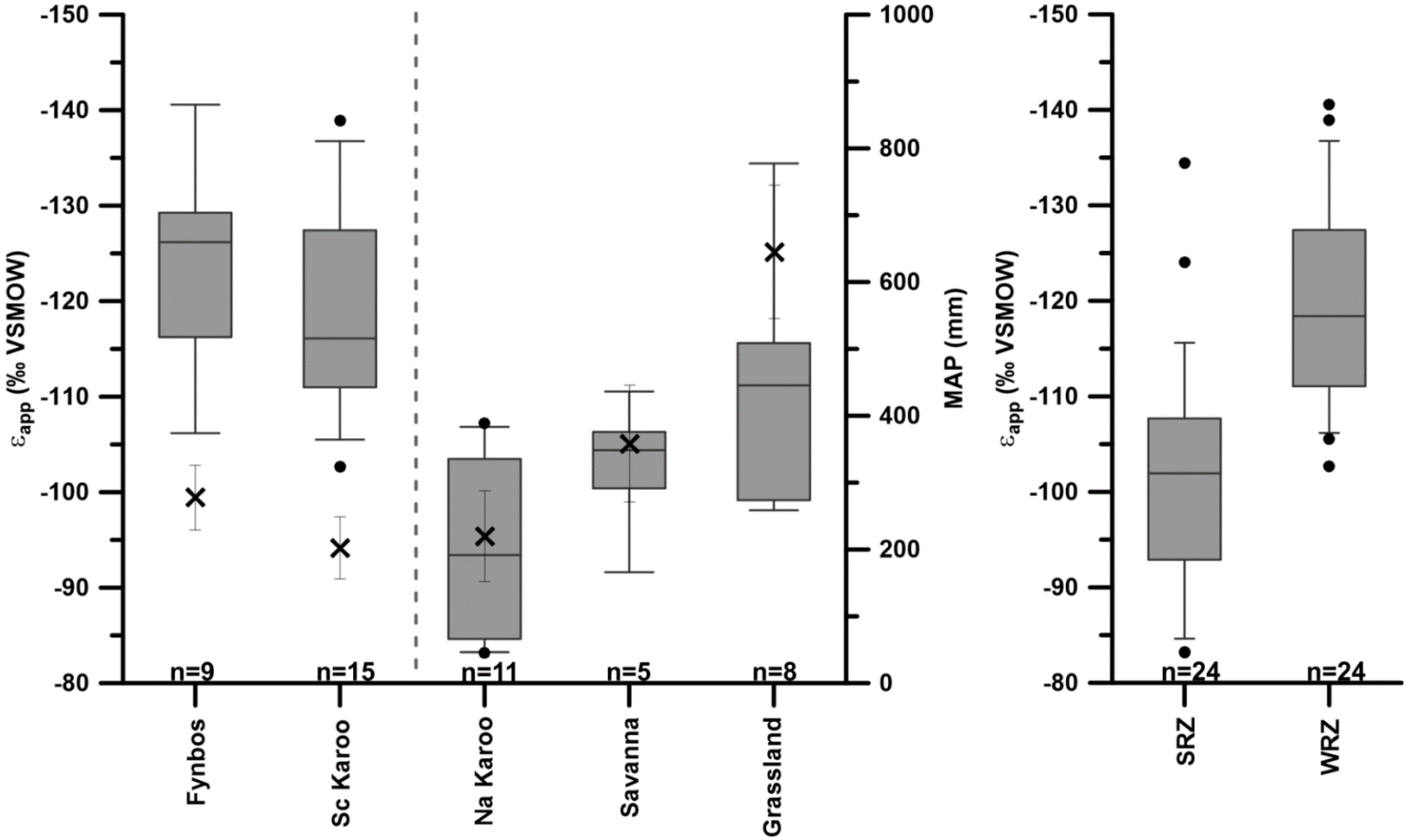

915 **Fig. 6.** Box and whisker plots for the apparent hydrogen isotope fractionation (ε_{app}) of plant wax derived *n*-alkanes in soils from different biomes (left)
916 and rainfall zones (right). Boxes comprise middle 50% of samples and the horizontal black line within the box represents the median. Black dots
917 outside the whisker plots indicate the uppermost and lowermost 10%. Na Karoo and Sc Karoo indicate Nama Karoo and Succulent Karoo,
918 respectively. Black crosses indicate the mean of mean annual precipitation (MAP) for each biome. Vertical dashed grey line separates WRZ
919 dominated biomes (Fynbos, Sc Karoo) from SRZ dominated biomes (Na Karoo, Savanna, Grassland). Note that ε_{app} is shown on an inverse axis.

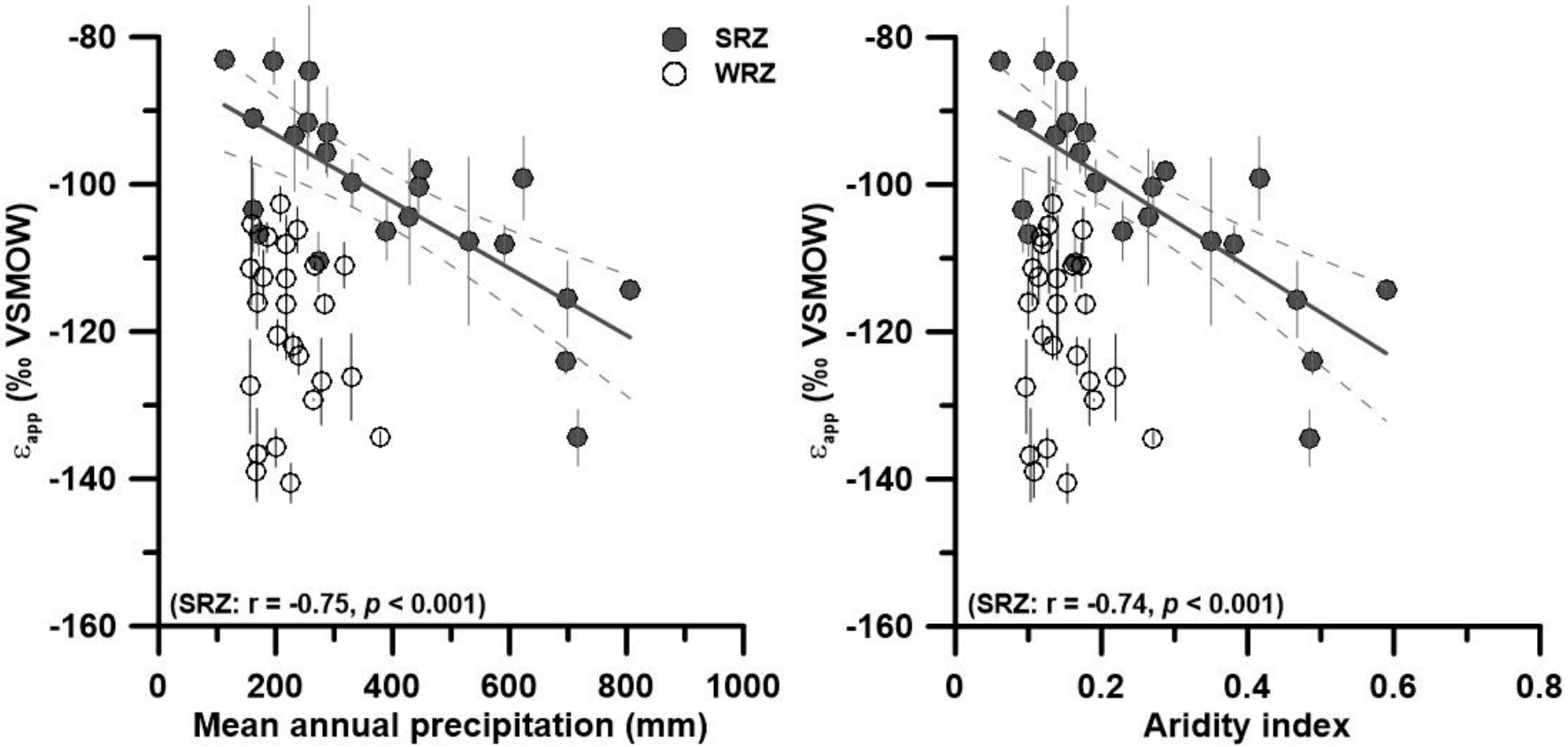

Fig. 7. Correlation of apparent hydrogen isotope fractionation (ε_{app}) with mean annual precipitation (left, Hijmans et al., 2005) and aridity index (right, Trabucco and Zomer, 2009) in South Africa divided into the summer rainfall (SRZ, grey dots) and winter rainfall zone (WRZ, open dots). Grey lines show linear fits and grey dashed lines 95% confidence intervals of the SRZ samples.

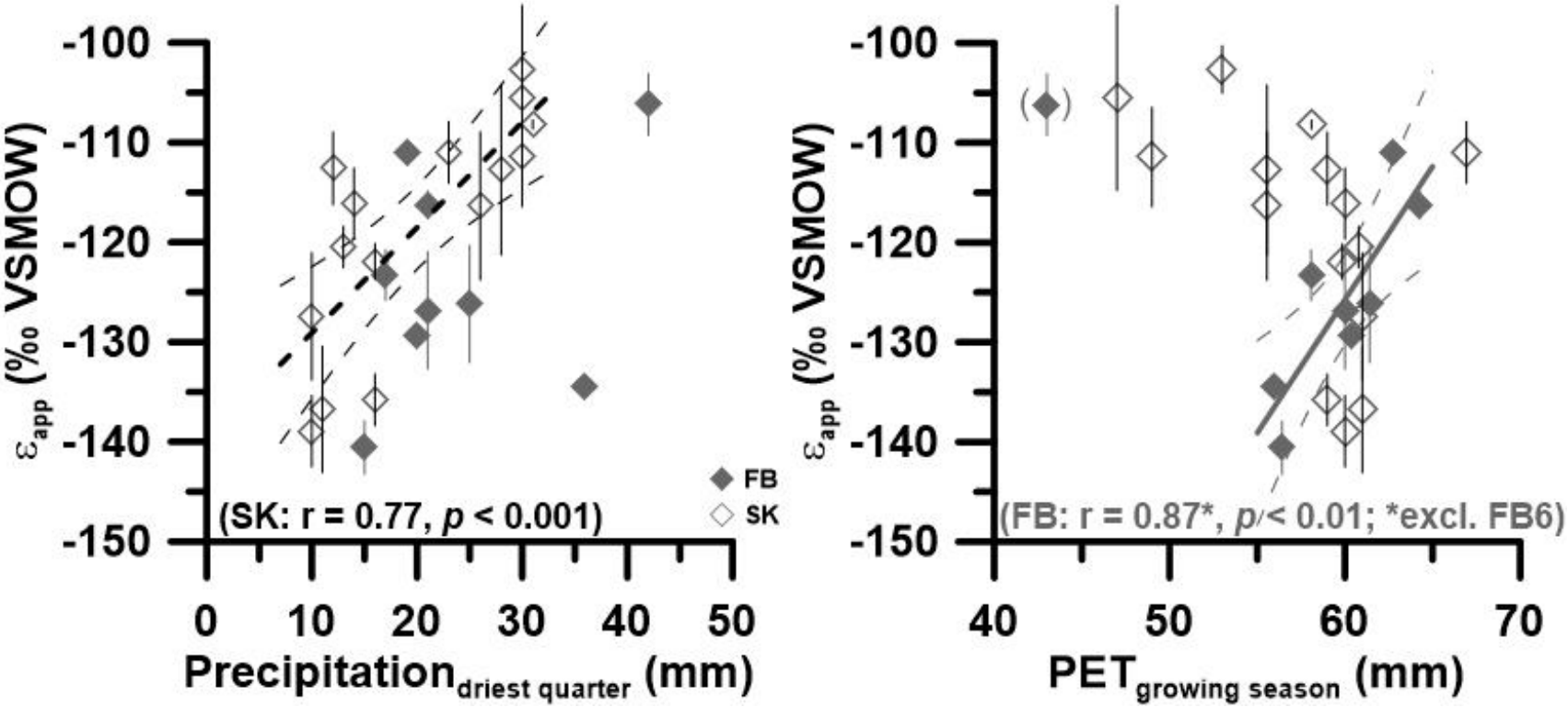

Fig. 8. Correlation of apparent hydrogen isotope fractionation (ε_{app}) with driest quarter precipitation (left) and growing season potential evapotranspiration (PET, right) in the WRZ divided into the Succulent Karoo (SK, grey open diamonds) and Fynbos (FB, grey diamonds) biomes. An outlier was excluded for the Pearson correlation coefficient between ε_{app} and PET of Fynbos soils. Linear fits and 95% confidence intervals are shown for SK soils (left) and FB soils (right), respectively.

930 **Table 1**

931 δD values (minimum, maximum and range) of precipitation, individual *n*-alkanes (C_{29}, C_{31}) and amount weighted mean of *n*-alkanes (C_{29} and C_{31}) in

932 the study area separated into different rainfall zones and biomes.

	δD_p (‰) annual (OIPC)			δD_{C29} (‰)			δD_{C31} (‰)			δD_{wax} (‰) weighted mean (C_{29} + C_{31})		
	min	max	range	min	max	range	min	max	range	min	max	range
Rainfall zone												
SRZ (n=21)	-36	-19	17	-151 ± 0	-75 ± 0	76	-161 ± 1	-111 ± 1	49	-157 ± 4	-108 ± 8	49
WRZ (n=21)	-25	-10	15	-146 ± 1	-82 ± 0	64	-163 ± 1	-120 ± 1	44	-163 ± 1	-120 ± 4	33
YRZ (n=6)	-28	-19	9	-136 ± 1	-83 ± 2	53	-135 ± 1	-105 ± 1	30	-132 ± 5	-106 ± 1	26
Biome												
Fynbos (n=9)	-24	-6	18	-146 ± 1	-121 ± 1	25	-163 ± 1	-125 ± 0	38	-163 ± 1	-125 ± 1	38
Succulent Karoo (n=15)	-23	-5	18	-142 ± 1	-82 ± 0	60	-156 ± 0	-120 ± 1	36	-154 ± 4	-121 ± 2	33
Nama Karoo (n=11)	-17	-10	-7	-117 ± 1	-75 ± 0	42	-134 ± 1	-105 ± 1	29	-133 ± 3	-106 ± 1	27
Savanna (n=5)	-16	-14	2	-119 ± 0	-103 ± 3	16	-141 ± 1	-123 ± 1	18	-141 ± 2	-118 ± 6	23
Grassland (n=8)	-31	-18	13	-151 ± 0	-112 ± 2	39	-161 ± 1	-129 ± 1	32	-157 ± 4	-128 ± 1	29

933

934 **Table 2**

935 Pearson correlation coefficients (r) between δD_{wax} and δD_p values of annual precipitation and precipitation
936 during the driest quarter for the different rainfall zones and biomes.

δD_{wax}	δD_p annual (‰ VSMOW)	δD_p driest quarter (‰ VSMOW)
All (n=48)	r = -0.12, *p* = 0.41	r = -0.09, *p* = 0.55
SRZ (n=21)	r = 0.65, *p* < 0.01	r = 0.12, *p* = 0.62
WRZ (n=21)	r = -0.48, *p* = 0.02	r = -0.48, *p* = 0.03
YRZ (n=6)	r = 0.82, *p* = 0.04	r = 0.93, *p* < 0.01
SRZ/YRZ[a] (n=24)	r = 0.66, *p* < 0.001	r = 0.09, *p* = 0.68
WRZ/YRZ[b] (n=24)	r = -0.48, *p* = 0.02	r = -0.52, *p* < 0.01
Fynbos (n=9)	r = -0.42, *p* = 0.26	r = -0.33, *p* = 0.38
Sc Karoo[c] (n=15)	r = -0.58, *p* = 0.03	r = -0.60, *p* = 0.02
Na Karoo[d] (n=11)	r = 0.02, *p* = 0.95	r = 0.22, *p* = 0.51
Savanna (n=5)	r = 0.22, *p* = 0.73	r = 0.02, *p* = 0.97
Grassland (n=8)	r = 0.34, *p* = 0.40	r = -0.16, *p* = 0.71

937 [a] For δD_{wax} SRZ/YRZ the locations CNT5, CNT6 and GTC30 (see Supplementary materials) from the
938 northern parts of the YRZ are included;
939 [b] for δD_{wax} WRZ/YRZ the locations FB6, SK11, SK12 and NK1 (see Supplementary materials) from the
940 southern parts of the YRZ are included;
941 [c] Succulent Karoo;
942 [d] Nama Karoo.
943

944 **Table 3**

945 Pearson correlation coefficient (r) between ε_{app} and $\delta^{13}C_{wax}$ as well as different environmental parameters for the rainfall zones (SRZ, summer rainfall

946 zone; WRZ, winter rainfall zone) and the individual biomes. Bold numbers represent significant correlation coefficients (Sc Karoo, Succulent Karoo; Na

947 Karoo, Nama Karoo; gs, growing season; qu, quarter).

	ε_{app} SRZ		ε_{app} WRZ		ε_{app} Sc Karoo		ε_{app} Fynbos		ε_{app} Na Karoo		ε_{app} Savanna		ε_{app} Grassland	
	r	*p*	r	*p*	r	*p*	r	*p*	r	*p*	r	*p*	r	*p*
$\delta^{13}C_{wax}$	-0.24	0.264	0.27	0.211	0.11	0.704	0.28	0.470	0.49	0.124	-0.22	0.729	-0.39	0.337
MAP	**-0.75**	**<0.001**	-0.12	0.540	0.28	0.322	-0.24	0.535	-0.07	0.84	-0.14	0.818	-0.66	0.074
Precip. gs	**-0.75**	**<0.001**	-0.24	0.247	0.14	0.620	-0.33	0.382	-0.12	0.729	0.15	0.810	-0.73	0.04
MAT	**0.68**	**<0.001**	-0.46	0.020	**-0.69**	**<0.01**	-0.35	0.351	0.31	0.364	0.34	0.579	0.60	0.112
Aridity index	**-0.74**	**<0.001**	-0.17	0.407	0.40	0.136	-0.31	0.423	-0.07	0.833	-0.13	0.839	-0.63	0.097
Altitude	-0.51	0.300	**0.62**	**<0.001**	**-0,69**	**<0.01**	0.42	0.262	-0.12	0.732	-0.25	0.686	-0.54	0.165
PET annual	**0.64**	**<0.01**	0.07	0.744	-0.33	0.23	0.26	0.495	-0.17	0.625	0.00	0.996	0.46	0.257
PET gs	-0.11	0.622	-0.37	0.066	-0.46	0.089	**0.87**[a]	**<0.01**[a]	0.46	0.151	-0.23	0.709	-0.66	0.07
Precipitation														
Driest qu.	**-0.55**	**<0.01**	**0.56**	**<0.01**	**0.77**	**<0.001**	0.36	0.344	-0.19	0.576	-0.14	0.819	-0.13	0.759
Wettest qu.	**-0.75**	**<0.001**	-0.38	0.058	-0.18	0.515	-0.43	0.250	-0.05	0.881	-0.15	0.814	-0.68	0.063
Warmest qu.	**-0.76**	**<0.001**	**0.53**	**<0.01**	**0.69**	**<0.01**	0.31	0.424	-0.03	0.936	-0.15	0.816	-0.67	0.068
Seasonality	0.23	0.290	**-0.67**	**<0.001**	**-0.67**	**<0.01**	-0.51	0.160	0.12	0.715	-0.04	0.950	-0.60	0.118
Temperature														
Annual range	0.49	0.018	**0.69**	**<0.001**	**0.64**	**0.01**	0.71	0.033	-0.18	0.605	-0.29	0.635	0.42	0.297
Min. coldest month	**0.74**	**<0.001**	**-0.66**	**<0.001**	**-0.74**	**<0.01**	-0.55	0.122	0.41	0.213	0.31	0.616	0.68	0.063

Max. warmest month	**0.72**	**<0.001**	0.05	0.813	-0.28	0.313	0.21	0.592	0.24	0.482	0.07	0.906	0.67	0.071

[a] Excluding location FB6 improved the correlation for “PET gs” , with location FB6: r -0.23, *p*0.56.